TARGETING METABOLIC PATHWAYS THROUGH PHARMACOLOGICAL AND CHEMOTHERAPEUTIC INTERVENTIONS TO IMPROVE TRIPLE-NEGATIVE BREAST CANCER THERAPY

Alyssa N. Ho

A thesis submitted to the faculty at the University of North Carolina at Chapel Hill in partial fulfillment of the requirements for the degree of Master of Science in the Department of Nutrition in the Gillings School of Global Public Health.

Chapel Hill
2021

Approved by:

Stephen D. Hursting

John E. French

Saame R. Shaikh

ABSTRACT

Alyssa N. Ho: Targeting Metabolic Pathways through Pharmacological and Chemotherapeutic Interventions to Improve Triple-Negative Breast Cancer Therapy
(Under the direction of Stephen D. Hursting)

Triple-negative breast cancers (TNBCs) are an aggressive breast cancer subtype with systemic chemotherapy as the only current treatment option. Metabolic reprogramming is key to tumor resistance to stressors including therapy. We hypothesized that targeting nutrient-sensing pathways through IGF-1R/IR and mTORC1 inhibition would increase efficacy of the platinum-based agent carboplatin and that autophagy underpins cell survival. We investigated combinatorial drug treatment effects on cytotoxicity, target inhibition, and mitochondrial function in MDA-MD-231 cells. IGF-1R/IR and mTORC1 inhibition with BMS-754807 and everolimus, respectively, increased the cytotoxicity of carboplatin while BMS-754807 interacted with the autophagy inhibitor chloroquine increasing growth inhibition. This work indicates that IGF-1R/IR and/or mTORC1 suppression is potentially synergistic with carboplatin in TNBC cells and suggests IGF-1R/IR inhibition can collaborate with autophagy inhibition to suppress TNBC growth. We conclude that inhibiting nutrient-sensing metabolic pathways with chemotherapy and/or autophagy inhibition warrants additional study as a strategy to improve response in women with TNBC.

ACKNOWLEDGEMENTS

I would like to thank Dr. Stephen Hursting for providing me the opportunity to conduct research in his laboratory. I am thankful for his support during my time in the laboratory — his passion for research has inspired me to continue cancer research in my future endeavors. I am especially grateful for the guidance and support of Dr. Michael Coleman who has been an extraordinary mentor from my very first day in the Hursting lab and has been patient in teaching me every research technique discussed in this thesis. He has dedicated countless hours of his time helping me develop this project despite the unforeseen circumstances the laboratory has faced this year. I am immensely thankful to Mike for his brilliance in designing experiments and assistance in overcoming any challenges I have faced this year. His love of science and genuine interest in developing young researchers is unparalleled, and I am thankful to have received his mentorship during my time in the Hursting laboratory. Further, I am grateful to our laboratory manager Erika Rezeli, not only for her dedication to ensuring the Hursting laboratory operates smoothly but also for her kindness and care for others. Even amidst a pandemic, Erika worked tirelessly to ensure all laboratory members were supported, and this project would not have been accomplished without her. Being a part of the Hursting laboratory has been an incredibly rewarding experience and I am thankful to have spent the past three years contributing to the laboratory's research.

TABLE OF CONTENTS

LIST OF FIGURES

LIST OF TABLES

LIST OF ABBREVIATIONS

AKT	RAC-alpha serine/threonine-protein kinase
AMPK	AMP-activated protein kinase
Atg	Autophagy-related genes
BC	Breast cancer
BECN1	Beclin 1
CQ	Chloroquine
CR	Caloric/calorie restriction
DEPTOR	DEP domain containing mTOR interacting protein
ER	Estrogen receptor
FEC	Fluorouracil, epirubicin, cyclophosphamide
HCQ	Hydroxychloroquine
HER-2	Human epidermal growth factor receptor 2
IF	Intermittent fasting
IL-6	Interleukin 6
IL-8	Interleukin 8
IR	Insulin receptor
IGF	Insulin-like growth factor
IGF-1R	Insulin-like growth factor 1
IGFBP	IGF binding protein
MAPK	Mitogen-activated protein kinase
mLST8	Mammalian lethal with Sec13 protein 8
mSIN1	Mammalian stress-activated protein kinase-interacting protein 1

mTOR	Mammalian target of rapamycin
mTORC1	Mammalian target of rapamycin complex 1
mTORC2	Mammalian target of rapamycin complex 2
NF-κB	Nuclear factor kappa B
PI3K	Phosphatidylinositol 3-kinase
PKA	Protein kinase A family kinase
PKC	Protein kinase C family kinase
PKG	Protein kinase G family kinase
PPP	Picropodophyllin
PR	Progesterone receptor
PRAS40	Proline-rich AKT substrate of 40 kDa
Protor-1/2	Protein observed with Rictor-1/2
RAPTOR	Regulatory associated protein with mTOR
Rictor	Rapamycin insensitive companion of mTOR
SK6	Ribosomal protein S6 kinase
SREBP1	Sterol regulatory element binding factor 1
TMRM	Tetramethylrhodamine methyl ester
TNBC	Triple-negative breast cancer
TNF-α	Tumor necrosis factor alpha

CHAPTER 1: INTRODUCTION

Triple Negative Breast Cancer Overview

In the United States, breast cancer (BC) is the most commonly diagnosed cancer and second leading cause of cancer death among women, with over 280,000 projected cases in 2021[1]. Approximately 30% of women with BC will develop metastases resulting in a 5-year relative survival rate of approximately 25% and a median overall survival period of approximately 24 months[2]. An aggressive breast cancer subtype, triple-negative breast cancer (TNBC), accounts for 10-20% of invasive BC cases and is defined by the absence of estrogen receptor (ER), progesterone receptor (PR), and human epidermal growth factor receptor 2 (HER-2)[3]. TNBC occurs more frequently in premenopausal young women under 40 years old and notably, incidence is disproportionately higher in Black women compared to White women[4,5]. Compared with other molecular BC subtypes, TNBC has a 40% mortality rate within the first five years of diagnosis and approximately 46% of patients with TNBC will develop distant metastasis, after which the median survival time is only 13.3 months[4]. Furthermore, the rate of relapse in patients with TNBC is 19-40 months compared to 35-67 months in patients with non-TNBC[4].

Because TNBC lacks ER, PR, and HER-2, there is a lack of targeted therapies available to patients, leaving chemotherapy as the standard approach for TNBC treatment, regardless of cancer stage[6,7]. Chemotherapeutic compounds include taxanes which prematurely stop mitosis and ultimately inhibit cell division, anthracyclines that

are derived from *streptomyces bacterium* and promote apoptosis, and cyclophosphamides that are alkylating agents that produce nitrogen mustard and have cytotoxic effects on tumor cells[4]. Growing evidence of TNBC's sensitivity to DNA-damaging agents has increased interest in the use of platinum-based compounds such as carboplatin or cisplatin that bind to DNA and induce double-stranded breaks[7]. These breaks ultimately damage DNA, inhibiting its replication and transcription, thereby inducing cell death[7]. However, a major clinical challenge is the development of resistance mechanisms in platinum-based chemotherapy treatment[8]. Though TNBC is often more sensitive to neoadjuvant chemotherapy compared to other subtypes, there is worse overall survival in patients with residual disease after neoadjuvant therapy.[9] As chemotherapy remains the standard-of-care treatment for TNBC patients regardless of BC stage, alternative strategies are urgently needed to target TNBC progression.

Signaling Mechanisms

The profound heterogeneity within TNBC complicates identification of specific oncogene drivers to develop targeted therapies against TNBC[7]. However, one potential target for treating TNBC is the phosphatidylinositol 3-kinase/RAC-alpha serine/threonine-protein kinase/mammalian target of rapamycin (PI3K/AKT/mTOR) cascade which plays a critical role in cell proliferation, survival, and metabolism and is frequently dysregulated in TNBC (**Fig. 1**)[10]. The stimulation of receptor tyrosine kinases such as insulin receptor (IR) and insulin-like growth factor 1 receptor (IGF-1R) triggers phosphorylation of insulin receptor substrate (IRS) proteins[11]. Furthermore, IGF-1/IGF-1R binding activates PI3K to produce lipid messengers that activate the AKT cascade and subsequently activate the mTOR pathway[11].

IGF-1 Signaling

Insulin-like growth factor (IGF) is a family of growth hormones that play a crucial role in normal human growth and development. The IGF family is composed of IGF-1 and IGF- 2, which bind to receptors IGF-1R and IGF-2R to activate various intracellular signaling cascades involved in cell proliferation, differentiation, and apoptosis[12,13]. Though its role in cancer progression has not been fully elucidated, IGF-1 signaling has been extensively implicated in cancer development and progression[12]. Specifically, IGF-1R plays a well-known role in anchorage-independent growth, a defining characteristic of malignant cancer cells[14]. In many cases of BC, IGF-1R levels are increased regardless of BC subtype[15]. Furthermore, greater than 50% of breast tumors have an active IGF-1R[11]. IGF-1R is structurally similar to IR, sharing 84% homology across tyrosine kinase domains[16]. High levels of IGF-1 activity have been shown in TNBC cell lines and these findings have increased efforts to target IGF-1R activity for TNBC therapy[17].

Early clinical trials focused on IGF-1R/IR inhibition proved ineffective as monotherapy. A phase II clinical trial investigating the use of AXL1717, a small-molecule modulator of IGF-1R signaling, on non-small cell lung cancer found AXL1717 did not demonstrate significant benefit on progression-free or overall survival when used as a monotherapy[18]. Similarly, another study investigating the use of linsitinib, another IGF-1R inhibitor, on patients with relapsed small-cell lung cancer, found that although its use was safe, linsitinib did not demonstrate any useful clinical activity[19].

mTOR Signaling

In response to nutrients and growth factors, the mammalian target of rapamycin (mTOR) functions to regulate cell growth and metabolism[20]. The mTOR complexes are downstream components of the PI3K/AKT pathway which forms two functionally distinct complexes: mTOR complex 1 (mTORC1) and mTOR complex 2 (mTORC2) that both play an important role in tumorigenesis[21].

mTORC1 is composed of several distinct components including mTOR, regulatory associated protein with mTOR (RAPTOR), and mammalian lethal with Sec13 protein 8 (mLST8), DEP domain containing mTOR interacting protein (DEPTOR), proline-rich AKT substrate of 40 kDa (PRAS40)[20]. mTORC1 is responsive to several factors including energy and oxygen levels, amino acids, and growth factors. When glucose and intracellular ATP levels are high, mTORC1 is active; conversely, low energy and ATP levels act as an mTORC1 inhibitor[22]. Through phosphorylation of its downstream targets, ribosomal protein S6 kinase 1 (S6K1) and Lipin1, mTORC1 activates sterol regulatory element binding factor 1 (SREBP1), a transcription factor involved in lipid synthesis[22]. A study conducted by Ricoult et al. in 2016 demonstrated that inhibition of mTORC1-mediated activation of SREBP1 led to stunted lipogenesis in BC cells, thus reducing cellular proliferation and tumor growth[23]. Additionally, mTORC1 is responsible for regulating protein synthesis and plays an overall important role in cell growth/metabolism[6,21].

Similar to mTORC1, mTORC2 contains mTOR, mLST8, and Deptor but is also comprised of rapamycin insensitive companion of mTOR (Rictor), mSIN1, and Protor-1/2[20,24]. Following treatment with neoadjuvant chemotherapy, TNBCs have displayed

amplification of Rictor in residual disease[22].Through phosphorylation of protein kinases belonging to the PKA/PKG/PKC (AGC) family, mTORC2 is involved in controlling cell proliferation/survival[20]. mTORC2 also plays a critical role in AKT activation which promotes cell survival and proliferation[20]. mTORC2 exists in a positive feedback loop with PI3K and AKT whereby the partial activation of PI3K and AKT promotes mTORC2 activation and subsequently fully activates AKT[25]. Furthermore, mTORC2 increases IGF-1R/IR phosphorylation[26].

Given mTOR's important role in cell growth and tumor progression, mTOR inhibitors have emerged as promising potential treatments in cancer therapy. These include rapamycin and everolimus, which allosterically inhibit mTORC1[27]. Everolimus has been approved for use in several cancers including BC[27]. However, because everolimus specifically targets mTORC1, its use as a monotherapy has been associated with resistance mechanisms[27,28].

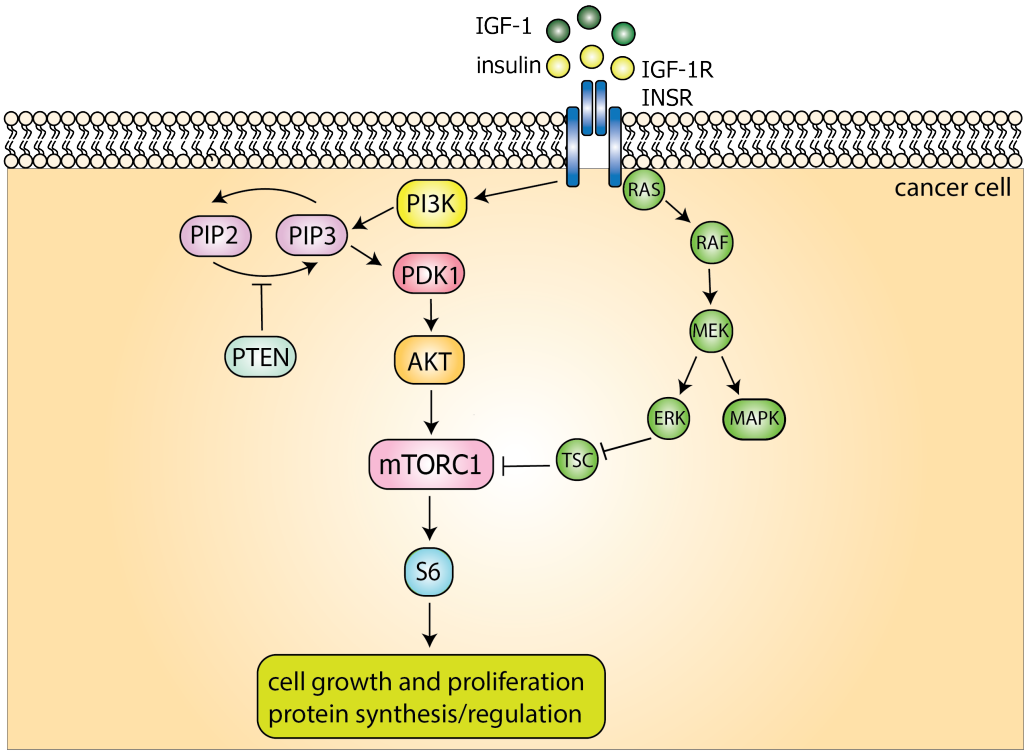

Figure 1. Activation of the PI3K/AKT/mTOR pathway is critical in TNBC. Binding of IGF-1/IR to receptors, IGF-1R and IR, triggers the MAPK and PI3K/AKT pathway, which then activates the downstream targets, mTORC1 and S6, ultimately leading to cell growth and proliferation and protein synthesis/regulation.

Obesity Increases Risk of Breast Cancer Development and Progression

Obesity is a major public health concern in the United States as it is projected that by 2030, half of the US population will be obese and nearly 25% of all adults will be severely obese[29]. Importantly, nearly 20% of U.S. cancer diagnoses are related to excess body weight[30]. Obese women represent a unique and expanding patient population as obesity is associated with worse outcomes in patients bearing BC, and obese patients are at greater risk of developing TNBC than non-obese women[31,32]. The negative outcomes associated with obesity and BC include not only increased mortality but also a shorter time to disease recurrence[33]. A 2015 study conducted by Copson et al. found that obese patients with BC, defined as having a BMI$\geq$30kg/m^2 had

significantly larger median tumor size compared to healthy weight individuals, defined as having a BMI<25kg/m^2[34]. Furthermore, the incidence of ER/PR/HER-2 negative tumors matching the TNBC subtype was 25.0% compared to 18.3% in healthy weight individuals[34].

There are several mechanisms by which obesity impacts BC initiation, progression, and metastasis including increased bioavailability of IGF-1 and increased stimulation of the PI3K/Akt/mTOR signaling pathway[35,36]. Obese patients often have some degree of insulin resistance and increased levels of circulating insulin as well as IGF-1 which contribute to a greater risk of developing BC[36]. Increased insulin levels can not only directly activate pro-growth signaling pathways but also reduce IGF binding protein (IGFBP), which binds to and inhibits IGF-1 under normal conditions. Thus, IGF-1 levels increase and as previously mentioned, bioavailable IGF-1 can bind to IGF-1R to trigger downstream signaling cascades such as the PI3K/AKT/mTOR pathway which promotes tumor growth and progression[37]. A study conducted by Chen et al. found that genetically obese or diet-induced obese mice injected with E0771 (basal-like) BC cells showed upregulated expression of mTOR in mammary tumors compared to mice fed a normal chow diet[38].

In addition to increasing insulin/IGF-1 levels, the obese state is also associated with increased preadipocyte formation which leads to higher leptin production that favors pro-tumorigenic angiogenesis and mitogenesis[33]. Increased adipokines in the obese state also promote inflammation primarily through the nuclear factor kappa B (NF-κB) pathway which activates gene expression encoding the pro-inflammatory cytokines: interleukin 6 (IL-6), interleukin 8 (IL-8) and tumor necrosis factor alpha (TNF-

α)[33,39]. These pro-inflammatory cytokines promote invasion and metastasis that contributes to poor patient outcomes in those with TNBC[39]. A study conducted by Hartman et al. in 2013 found that inhibition of IL-6 and IL-8 in MDA-MB-231 cells, a model of TNBC, resulted in significantly decreased anchorage-independent colony formation[40].

Thus, obesity promotes TNBC progression via numerous tumor cell intrinsic and extrinsic mechanisms. As obesity incidence in the U.S. continues to rapidly increase, these factors emphasize a need for treatments to specifically target obesity related TNBC progression.

Nutrient Restrictive Interventions and Metabolic Reprogramming in Breast Cancer

A growing area of nutrition and cancer research, with the potential to improve cancer outcomes is dietary modification such as calorie restriction (CR) and intermittent fasting (IF). Though these two dietary modifications both provide several beneficial effects resulting in extended lifespan and delayed onset of age-related disorders, they elicit distinct effects on normal and tumor cells[41]. CR is commonly defined in mouse models as a reduction (~30%) in total caloric intake without risk of developing malnutrition whereas IF is defined as the total avoidance of calories for a defined period of time[41,42].

The use of CR has extensively been shown to induce antitumorigenic effects in rodent models of BC[41]. Moreover, parallel studies investigating the use of CR diet in rhesus monkeys showed a significant reduction cancer incidence in monkeys fed a CR diet compared to control diet thus providing promising evidence that the benefits associated with CR are translatable to humans[43]. There are several mechanisms by

which CR mediates its beneficial effects including decreased growth factor and anabolic hormone production, especially IGF-1, as well as a reduction in pro-inflammatory cytokines and leptin production[41,44]. The Hursting lab has previously investigated the effects of CR on IGF-1 response in a murine model of colon cancer[44]. Female C57BL/6 mice randomized to receive a 30% CR or control diet were injected with MC38 colon tumor cells. Mice fed the CR diet not only showed decreased body fat/weight and tumor incidence but also showed lower levels of serum IGF-1 and insulin. Further analysis of tumors from CR mice revealed decreased expression of the pro-inflammatory cytokines IL-6 and TNF-α[44].

In contrast to CR, in which there is a chronic calorie deficit, IF results in the depletion of glycogen stores from the liver to provide energy. When glycogen stores are emptied, the body relies on the catabolism of amino acids and fatty acids to provide energy in the form of glucose and ketone bodies[45]. Like CR, IF also results in reduced IGF-1 levels, mediated by increased circulating IGFBP-1, which binds to IGF-1 preventing its interaction with IGF-1R[46]. Data suggests that IF results in greater reduction of glucose levels compared to those associated with CR[47]. IF also results in decreased circulating leptin, which is a hormone that inhibits hunger but causes an increase in adiponectin, which results in increased breakdown of fatty acids[46]. The beneficial effects of IR have also been shown to increase sensitization to some chemotherapeutic agents in preclinical TNBC murine models. A study conducted by de Groot et al. in 2015 investigated the effects of short-term fasting (24 hours) before and after receiving (neo)-adjuvant TAC (docetaxel/doxorubicin/cyclophosphamide) on patients with early-stage BC. They concluded that short-term fasting during

chemotherapy was well tolerated and reduced the hematological toxicity of TAC in HER2-negative BC patients[48].

While dietary interventions in the form of CR and IF have shown beneficial effects in preclinical murine models, there remain challenges in translating to cancer patients[45]. It is difficult to translate CR interventions from mice to humans, and there are concerns about the feasibility of implementing such extreme diets in patients due to the potential weight loss and discomfort that may result[45,49]. Because of these concerns, there is interest in identifying pharmacologic approaches, or metabolic reprogramming interventions (MRIs), which can be combined in innovative ways to recapitulate some or most of the beneficial effects of CR but with fewer challenges impacting adherence. Targets of the IGF-1 and AKT/mTOR pathways are of particular interest due to the role of these pathways in mediating CR and IF's anticancer effects[50].

The FDA-approved everolimus (formerly called RAD001), an analog of rapamycin, is a pharmacological agent that works as an mTORC1 inhibitor (**Fig. 2**). Everolimus is currently being tested in several clinical trials and has been approved for use in the treatment of refractory renal cell carcinoma and pancreatic neuroendocrine tumors as well as some BCs[51–53]. The use of everolimus in TNBC therapy is limited but a study conducted by Yunokawa et al. in 2012 investigated the effect of everolimus in a nine TNBC cell lines. The results showed that everolimus inhibited cell growth *in vitro* in five of the nine TNBC cell lines[54]. Furthermore, this study investigated the effects of everolimus *in vivo* in a mouse xenograft model of TNBC using MDA-MB-231 and MDA-MB-468 cells. Mice were treated with everolimus three times per week for three weeks, and the results showed that everolimus significantly reduced tumor volume of the MDA-

MB-468 but not the MDA-MB-231 xenografts[54]. Although everolimus has demonstrated growth inhibitory effects, it is generally ineffective when used alone in treatment of TNBC (need ref), and further experimentation is needed to fully understand ways to enhance its beneficial effects.

In addition to everolimus, BMS-754807 which works as a reversible dual small-molecule inhibitor of both IGF-1R and IR, provides another promising option as a mimetic of the beneficial antitumor effects of CR (**Fig. 2**). In preclinical trials, BMS-754807 has demonstrated efficacy *in vitro* for the treatment of a variety of human cancers including BC, pancreatic, colon, and lung cancer[55]. A 2012 study conducted by Awasthi et al. studied the combination of gemcitabine, a DNA synthesis inhibitor and BMS-754807 in mice injected with human pancreatic ductal adenocarcinoma (PDAC) xenografts. The results showed that while gemcitabine treatment alone inhibited the growth of PDAC xenografts, BMS-754807 enhanced the gemcitabine inhibitory response[56]. Although numerous clinical trials have made use of IGF-1/IGF-1R inhibitors, they have not demonstrated much benefit when used as single agents (ref). Thus, the ability of pharmacological agents to target IGF-1 and mTORC1 provides a promising treatment option, but one needs to be further explored especially with regard to TNBC.

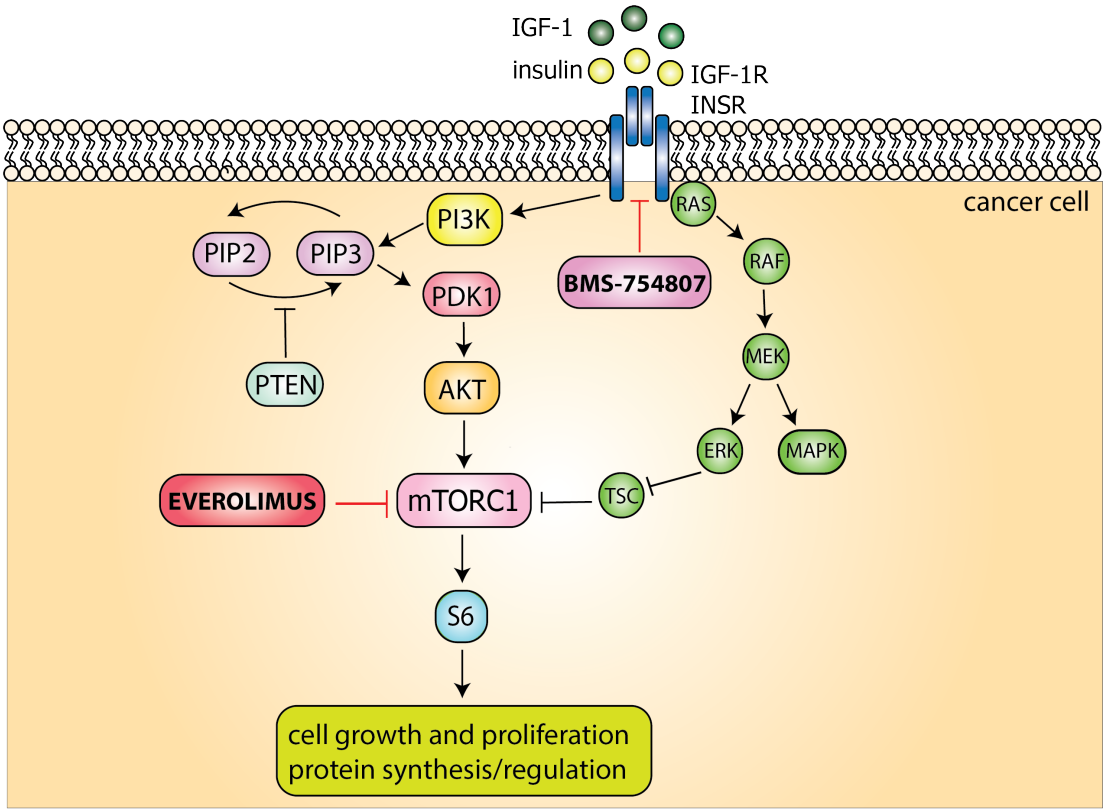

Figure 2. PI3K/AKT/mTOR signaling can be inhibited by everolimus or BMS-754807.
BMS-754807 works as a dual small-molecule inhibitor of both IGF-1R and IR while everolimus works as an mTORC1 inhibitor.

Autophagy's Role in Cancer

Autophagy is a highly conserved cellular process involved in the degradation of cellular material that can subsequently be recycled to provide energy for the cell[57]. This thesis will focus on the most well-studied form of autophagy, macroautophagy (hereafter referred to as autophagy), in which cellular contents are first sequestered in double-membrane-bound vesicles known as autophagosomes, a process regulated by autophagy-related genes (Atg)[58,59]. The autophagosomes fuse with lysosomes forming autolysosomes whose contents are degraded and recycled[58]. Autophagy is predominantly regulated by AMP-activated protein kinase (AMPK) and mTOR, downstream of the PI3K/AKT signaling cascade, which plays a major role in cellular

energy balance[60,61]. When nutrients are plentiful and energy stores are high, mTOR works to inhibit autophagy[57]. Conversely, during times of nutrient depletion or starvation, AMPK is activated while mTOR is inhibited due to less glucose transport and amino acid availability resulting in induction of autophagy[41,57]. Thus, under CR conditions, autophagy is a key homeostatic process necessary for removing damaged or redundant organelles, which in turn generates metabolites for energy or macromolecule production[41]. A 2016 study conducted by Pietrocola et al. investigated the effects of caloric restriction mimetics defined as pharmacological agents that reduce protein acetylation to increase autophagic activity on autophagy induction. They found that hydroxycitrate, an over-the-counter weight loss agent mimicking CR, induced autophagy *in vivo* in mice when injected[62].

In cancer, autophagy's role is complex, and its effects vary depending on the stage of cancer progression[59]. In the early stages of tumorigenesis, deletion of beclin 1 (BECN1), a protein necessary for autophagy induction, tumor induction/progression has been shown to be enhanced[58,59]. However, in established tumors, autophagy can be upregulated to protect against and overcome various cellular stressors and promote tumor progression[63,64]. As tumors continue to grow, cells located centrally within the tumor often experience dysfunctional vascularization; thus, autophagy acts as a compensatory mechanism allowing cancer cells to generate metabolic fuels to survive in hypoxic or low-nutrient environments[58].

Autophagy's ability to promote growth in established tumors provides a compelling argument for investigating the use of autophagy inhibition in cancer therapy, especially when considering that many current cancer treatments induce metabolic

stress that upregulates autophagy. Furthermore, as previously mentioned, CR results in an increased dependence on autophagy that, when combined with autophagy inhibition, may result in reduced tumor burden. The Hursting lab has previously investigated the use of autophagy inhibition alone and in combination with CR on Ras-driven tumors and found that combining a CR diet with autophagy inhibition resulted in greater tumor suppression than either CR or autophagy inhibition alone[65]. Many preclinical studies have also investigated the potential for exploiting increased autophagic activity under conditions of metabolic stress to improve the efficacy of autophagy inhibitors and existing chemotherapies. These studies commonly utilize the FDA-approved chloroquine (CQ) or hydroxychloroquine (HCQ), which work as autophagy inhibitors through deacidification of the lysosome to block autophagosome-lysosome fusion[57]. One of the first studies to demonstrate the ability of autophagy inhibition to enhance the anticancer effects of other therapies was a 2007 study conducted by Amaravadi et al. that utilized a Myc-induced model of lymphoma whose p53 mutant tumor cells were resistant to apoptosis. Treatment with tamoxifen resulted in p53 reactivation with increased apoptosis as well as the induction of autophagy. Subsequent inhibition of autophagy via CQ treatment or ATG5 shRNAs in combination with alkylating agents resulted in increased cell death[66].

The potential for autophagy inhibitors such as CQ to further enhance anticancer therapies provides a rationale for further investigating the use of CQ in combination with chemotherapy or pharmacological agents associated with growth factor signaling (mTOR) inhibition. Although chemotherapy is the standard-of-care treatment for patients with TNBC, many patients will develop resistance to treatment and CQ has shown

promise in overcoming chemotherapeutic resistance[67]. A 2014 study conducted by Chittaranjan et al. investigated the effects of combining the anthracycline, epirubicin, with HCQ treatment in both epirubicin-resistant and sensitive TNBC cells. The combination of epirubicin with HCQ increased therapeutic efficacy and also resulted in significantly reduced tumor growth compared to either epirubicin or HCQ treatment alone[68].

Given the importance of nutrient-sensing pathways including IGF-1 and mTOR on the tumor environment and its metabolic responses, this thesis proposes the use of pharmacological compounds to treat TNBC, termed metabolic reprogramming interventions, in combination with traditional cytotoxic platinum chemotherapy. Identification of pharmacological approaches that recapitulate the beneficial biochemical effects of dietary energy restriction has the potential to improve current TNBC treatment by increasing the efficacy of existing chemotherapy treatments. We will also investigate the effects of combining CQ with the aforementioned pharmacological agents, BMS-754807 and everolimus. We hypothesized that inhibition of the IGF-1R/IR and mTORC1 pathways by BMS-754807 and everolimus, respectively, stimulates autophagy and thus, combining these agents with CQ or carboplatin could potentially block the survival mechanism of TNBC cells.

Project Goals

The goals of the project are as follows: 1) Determine whether metabolic reprogramming via IGF-1R/IR or mTORC1 inhibition enhances TNBC response to platinum chemotherapy. 2) Determine whether metabolic reprogramming interventions

promote autophagy and if autophagy underpins survival following IGF-1R/IR or mTORC1 inhibition.

CHAPTER 2: METABOLIC REPROGRAMMING INTERVENTIONS INHIBITING IGF-1R/IR OR MTORC1 ENHANCE RESPONSE TO PLATINUM CHEMOTHERAPY

Methods

Cell Lines Used

The human breast cancer cell line, MDA-MB-231 (ATCC HTB-26) derived from breast adenocarcinoma, was cultured in Dulbecco's Modified Eagle Medium (DMEM) containing 4.5g/L glucose supplemented with 10% fetal bovine serum (FBS) and 2mM L-glutamine. Cells were maintained at 37ºC in a humidified 5% CO_2 chamber.

MTT Assay

MDA-MB-231 cells were seeded ($1x10^4$ cells/well) in a 96-well plate overnight in glucose-restricted (1g/L) media for 24 hours, then treated with either everolimus or BMS-754807 across a range of doses for 24 hours, and finally treated with carboplatin for an additional 48 hours resulting in a 72-hour total treatment time. Media was aspirated and cells were incubated in a solution containing 3-(4,5-dimethylthiazol-2-yl)-2,5-diphenyltetrazolium bromide (MTT) (0.5mg/mL) in PBS. After 1.5 hours. MTT reagent was removed and cells and precipitate solubilized with dimethyl sulfoxide (DMSO) and agitated on a plate shaker for 10 minutes. Absorbance was measured at 570 and 690 nm via a Cytation 3 Cell Imaging Reader (BioTek).

Western Blotting

To confirm target inhibition following treatment with BMS-754807 or everolimus, MDA-MB-231 cells ($2.1x10^6$ cells/plate) were seeded into 10cm plates to achieve 70%

confluency after 24 hours. Cells were then treated with low-glucose (1g/L) DMEM containing either everolimus (15.63nM) or BMS-754807 (5μM). After treatment for 4 hours, whole cell lysates were generated using radioimmunoprecipitation (RIPA) buffer supplemented with protease inhibitor cocktail (Sigma Aldrich) and phosphatase inhibitors (sodium orthovanadate, sodium pyrophosphate, β-Glycerophosphate). Cells were scraped from plates, incubated on ice for 20 minutes, and centrifuged at 24,000 rcf for 15 minutes at 4°C. The protein-containing supernatant was collected, and a Bradford assay (BioRad) was performed to determine protein concentration. Equal amounts of protein were added to solution containing 5X Loading Buffer (BioRad) and 5% β-mercaptoethanol. Protein was then separated via SDS-PAGE and transferred to PVDF membrane (Bio-Rad). Membranes were blocked with 5% bovine serum albumin (BSA) in Tris Buffered Saline with 0.1% Tween (TBST) for 1 hour before being incubated overnight at 4°C with primary antibody. After washing with TBST, membranes were blocked in secondary IRDye 680 RD goat anti-mouse (LI-COR #926-68070, 1:10000) or IRDye 800CW goat anti-rabbit antibody (LI-COR #926-32211, 1:10000) for 1 hour at room temperature. Excess secondary antibody was removed by TBST washes. Antibody binding was detected with the Odyssey Imaging System (LI-COR). Images were analyzed via near-infrared fluorescence using Image J software according to NIH gel analysis procedures[69]. The following primary antibodies were used: p-AKT S473 (CST #4060S, 1:1000), Akt (CST #9272S, 1:1000), pIGF-1R (CST #3918S, 1:1000), IGF-1R (CST #3027S, 1:1000), p-S6 Ser 235/236 (CST #2211S, 1:1000), S6 (CST #2317, 1:1000), β-Actin (Santa Cruz Biotechnology #sc-47778, 1:5000).

Flow Cytometry

MitoSOX Red mitochondrial superoxide indicator

MDA-MB-231 cells were seeded ($4.25x10^5$ cells/well) in a 6-well plate overnight in low-glucose (1g/L) media, then treated with BMS-754807 (2.5μM) or everolimus (15.63nM) for 4 hours. Cells were then trypsinized (Trypsin-EDTA, 0.25%, Gibco) and stained using MitoSOX red mitochondrial superoxide indicator (Invitrogen #M36008, 1:500) diluted in FACS buffer ± Menadione dye (Sigma Aldrich #M5625, 1:1000), ± Zombie NIR Fixable Viability Kit (BioLegend #B331244, 1:600). Following 30 minutes of staining, data was acquired using a CytoFLEX flow cytometer (Beckman Coulter). Laser excitation at 488 nm was used to capture 10,000 single cell live events for each sample.

MitoTracker Green FM indicator

MDA-MB-231 cells were seeded ($3.9x10^5$ cells/well) in a 6-well plate overnight in low-glucose (1g/L) media, then treated with BMS-754807 (2.5μM) or everolimus (15.63nM) for 24 hours. Cells were then trypsinized (Trypsin-EDTA, 0.25%, Gibco) and stained using MitoTracker Green FM indicator (Invitrogen #M36008, 1:2000) diluted in FACS buffer ± Zombie NIR Fixable Viability Kit (BioLegend #B331244, 1:600). Following 30 minutes of staining, data was acquired using a CytoFLEX flow cytometer (Beckman Coulter). Laser excitation at 488 nm was used to capture 10,000 single cell live events for each sample.

TMRM indicator

MDA-MB-231 cells were seeded ($4.25x10^5$ cells/well) in a 6-well plate overnight in low-glucose (1g/L) media, then treated with BMS-754807 (2.5μM) or everolimus (15.63nM) for 4 hours. Cells were then trypsinized (Trypsin-EDTA, 0.25%, Gibco) and

stained using TMRM reagent (Sigma Aldrich #T5428, 1:5000) diluted in FACS buffer ± FCCP reagent (Sigma, 10nM), ± Zombie NIR Fixable Viability Kit (BioLegend #B331244, 1:600). Following 30 minutes of staining, data was acquired using a CytoFLEX flow cytometer (Beckman Coulter). Laser excitation at 488 nm was used to capture 10,000 single cell live events for each sample.

Statistical Analysis

Data were analyzed using GraphPad Prism 8 software (GraphPad Software, Inc.). Additionally, SynergyFinder software was utilized to determine synergy via the Bliss independence model. Differences between means were assessed via one-way analysis of variance (ANOVA) with Tukey's multiple comparisons for statistical differences. Differences were considered significant at $p<0.05$. Data graphically presented as mean ± standard error of mean (SEM) unless otherwise noted.

Results

Metabolic reprogramming via BMS-754807 or everolimus reduced cellular viability of human-derived triple-negative breast cancer cells

To determine whether metabolic reprogramming interventions inhibited triple-negative BC cell growth, we tested the effects of the dual IGF-1R/IR inhibitor, BMS-754807, and the mTORC1 inhibitor, everolimus, on the viability of MDA-MB-231 TNBC cells cultured under low-glucose (1g/L) conditions, for 24 hours. Low-glucose media was used for experimental analyses to model and investigate response to therapies under conditions consistent with homeostatic glucose levels in a normoglycemic individual. Cellular viability was assessed via MTT viability assay which measures the reduction of a yellow tetrazolium salt to purple formazan crystals to quantify the amount of metabolically active cells[70]. Following 24 hours of treatment with BMS-754807, MDA-

MB-231 cells cultured in low-glucose media showed significant growth inhibition at doses ≥2.5 μM ($p<0.01$ at 2.5μM, $p<0.001$ at 5μM) compared to control levels (**Fig. 3A**). Treatment with everolimus induced significant growth inhibition at doses ≥15.63nM ($p<0.001$ at 15.63nM, $p<0.01$ at 31.25nM, 62.5nM, and 125nM, $p<0.05$ at 250nM) compared to control levels (**Fig. 3B**). These results may be due to the overall limited growth inhibition of everolimus in the MDA-MB-231 cells. However, these results indicate that both BMS-754807 and everolimus have significant cytotoxic effects in MDA-MB-231 TNBC cells.

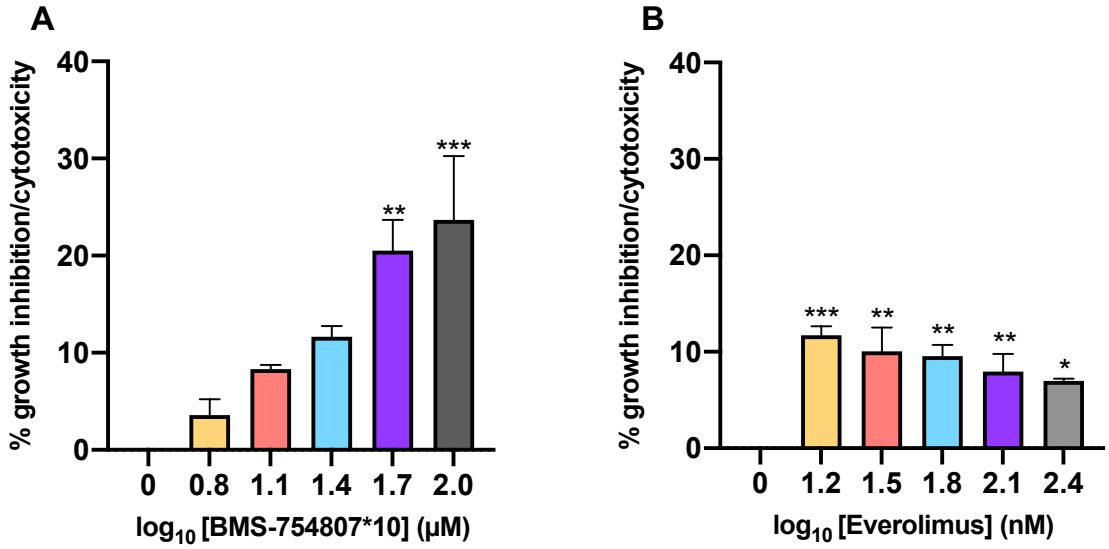

Figure 3. MRIs alone are cytotoxic in MDA-MB-231 cells.
Following 24 hours of culture in low-glucose (1g/L) media, MDA-MB-231 cells were treated with BMS-754807 at increasing doses of 0.625, 1.25, 2.5, 5 ($p<0.01$), and 10μM ($p<0.001$) **(A)** or everolimus at increasing doses of 15.63 ($p<0.001$), 31.25, 62.5, 125 ($p<0.01$), and 250nM ($p<0.05$) **(B)** for 24 hours. An MTT assay was conducted to measure % growth inhibition/cytotoxicity. Data presented as mean ± SEM for n=3 experiments.

Metabolic reprogramming interventions inhibited anticipated metabolic targets

To confirm that everolimus and BMS-754807 treatment inhibited the metabolic signaling pathways they target, western blotting was performed to examine the amount

of downstream protein targets following 4-hour incubation with each compound. Stimulation of IGF-1R activates the PI3K/AKT pathway[11]. Treatment with the dual IGF-1R/IR inhibitor BMS-754807 (5μM) resulted in decreased phosphorylation of AKT in MDA-MB-231 cells ($p<0.01$) (**Fig. 4A**), indicating that the selected dose of BMS-754807 is effective in impairing the IGF-1R/IR pathway. Furthermore, treatment with the mTORC1 inhibitor, everolimus (15.63nM) resulted in significantly decreased phosphorylation of ribosomal protein S6 (pS6) ($p<0.0001$) (**Fig. 4B**). Treatment with BMS-754807 also reduced pS6 levels ($p<0.05$) (**Fig. 4B**). Activated mTOR leads to the phosphorylation of S6; thus, these results indicate that the selected dose of everolimus effectively impairs downstream targets of the mTORC1 signaling pathway.

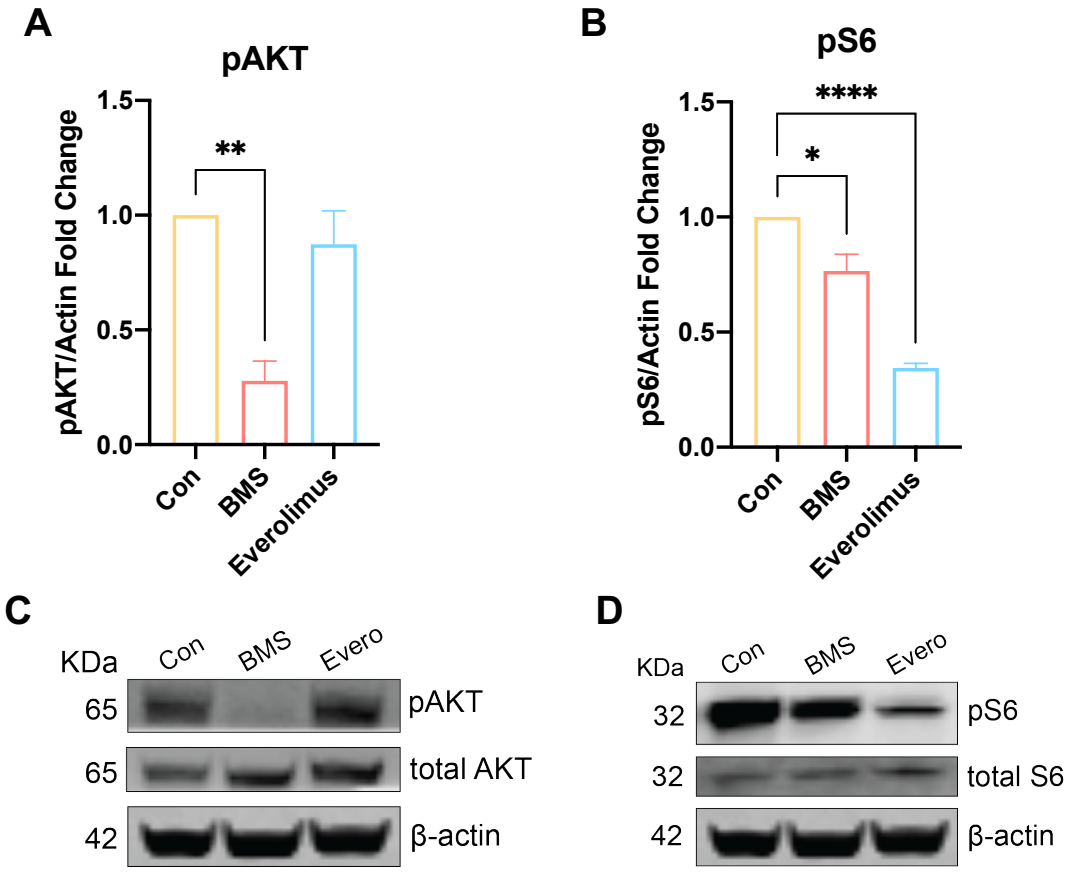

Figure 4. MRIs inhibited anticipated metabolic targets.
Confirmation of target inhibition in MDA-MB-231 cells treated with BMS-754807 and everolimus for 4 hours. Vector treatment with dimethyl sulfoxide (DMSO) serves as control for all experiments. Protein abundance was normalized to β-Actin loading control. Expression of pAKT **(A)**, pS6 **(B)** analyzed. Representative western blots from n=3 experimental replicates for pAKT/AKT **(C)** and pS6/S6 **(D)**. Data presented as mean ± SEM.

Mitochondria and reactive oxygen species analysis

To analyze mitochondrial mass following treatment of MDA-MB-231 TNBC cells with BMS-754807 or everolimus, cells were stained with MitoTracker Green FM which is a probe that fluoresces more brightly in active mitochondria compared to apoptotic mitochondria, thus measuring mitochondrial mass[71]. Staining with MitoTracker Green FM revealed a significant increase ($p<0.01$) in mitochondrial mass in MDA-MB-231 cells

treated with BMS-754807 compared to control and observed no difference in cells treated with everolimus (**Fig. 5A-B**).

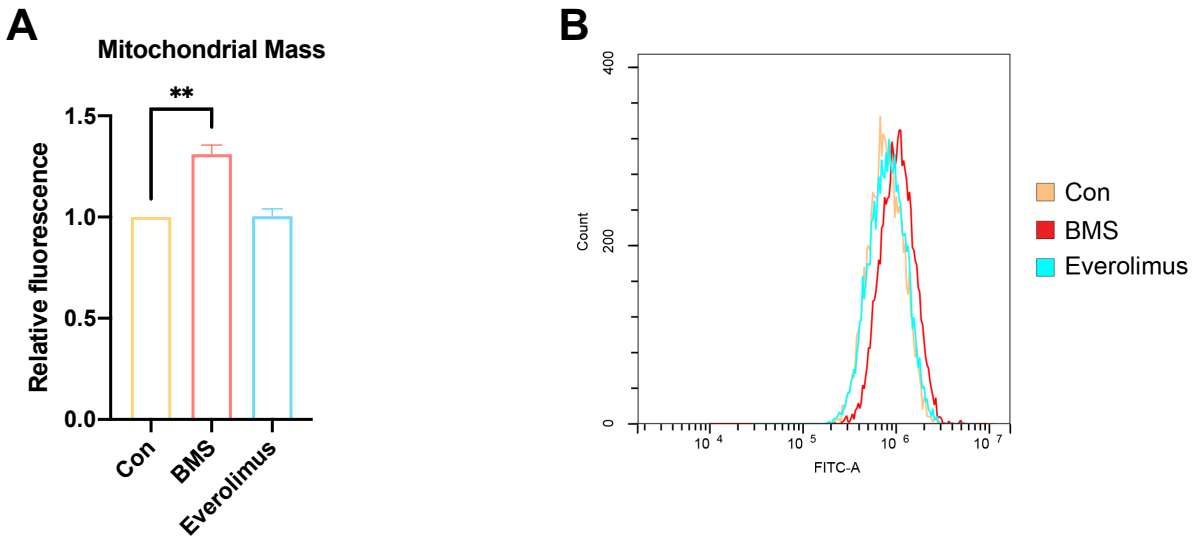

Figure 5. BMS-754807 treatment increased mitochondrial mass.
Following 24 hours of culture in low-glucose (1g/L) media, MDA-MB-231 cells were treated with BMS-754807 (2.5μM) or everolimus (15.63nM) for 24 hours before being stained with MitoTracker Green FM. Median fluorescence intensity **(A)** with representative frequency histogram of cellular fluorescence; lower fluorescence indicates smaller mitochondrial mass **(B)**. Data presented as mean ± SEM for n=3 experiments.

Next, to analyze mitochondrial superoxide production following treatment of MDA-MB-231 cells with BMS-754807 or everolimus, cells were stained with MitoSOX Red Reagent, a probe whose fluorescence increases as the concentration of superoxide increases[72]. There was no significant increase in mitochondrial superoxide production following treatment with either BMS-754807 or everolimus (**Fig. 6A-B**). We confirmed the functioning of the assay by treating cells with 50μM menadione for 30 min to confirm induction of signal (**Fig. 6C-D**).

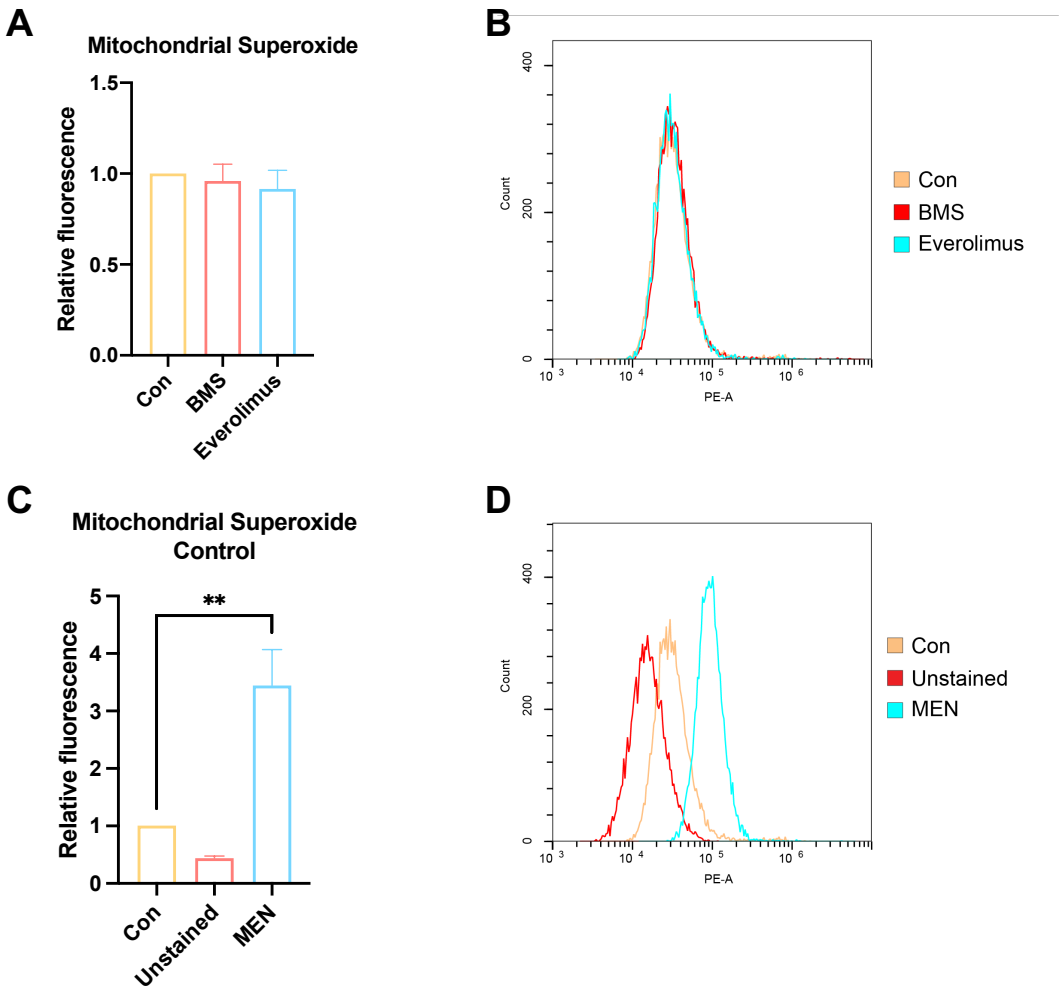

Figure 6. MRIs did not affect mitochondrial superoxide production. Following 24 hours of culture in low-glucose (1g/L) media, MDA-MB-231 cells were treated with BMS-754807 (2.5μM) or everolimus (15.63nM) for 4 hours before being stained with MitoSOX Red Reagent. Median fluorescence intensity **(A)** with representative frequency histogram of cellular fluorescence; increased fluorescence indicates increased concentration of superoxide **(B)**. Mitochondrial superoxide positive control achieved via menadione (MEN) treatment combined with MitoSOX Red Reagent **(C)** with representative frequency histogram of cellular fluorescence **(D).** Data presented as mean ± SEM for n=3 experiments.

Finally, to analyze mitochondrial membrane potential following treatment of MDA-MB-231 cells with BMS-754807 or everolimus, cells were stained with tetramethylrhodamine methyl ester (TMRM), a dye which fluoresces brightly and accumulates in healthy functioning mitochondria proportional to polarization, thus signal dims as the mitochondrial membrane potential is lost[73]. Once again, there was no

significant difference in mitochondrial membrane potential following treatment with either BMS-754807 or everolimus (**Fig. 7A-B**). We confirmed the functioning of the assay by treating cells with 50μM FCCP for 30 min and confirming suppression of signal (**Fig. 7C-D**).

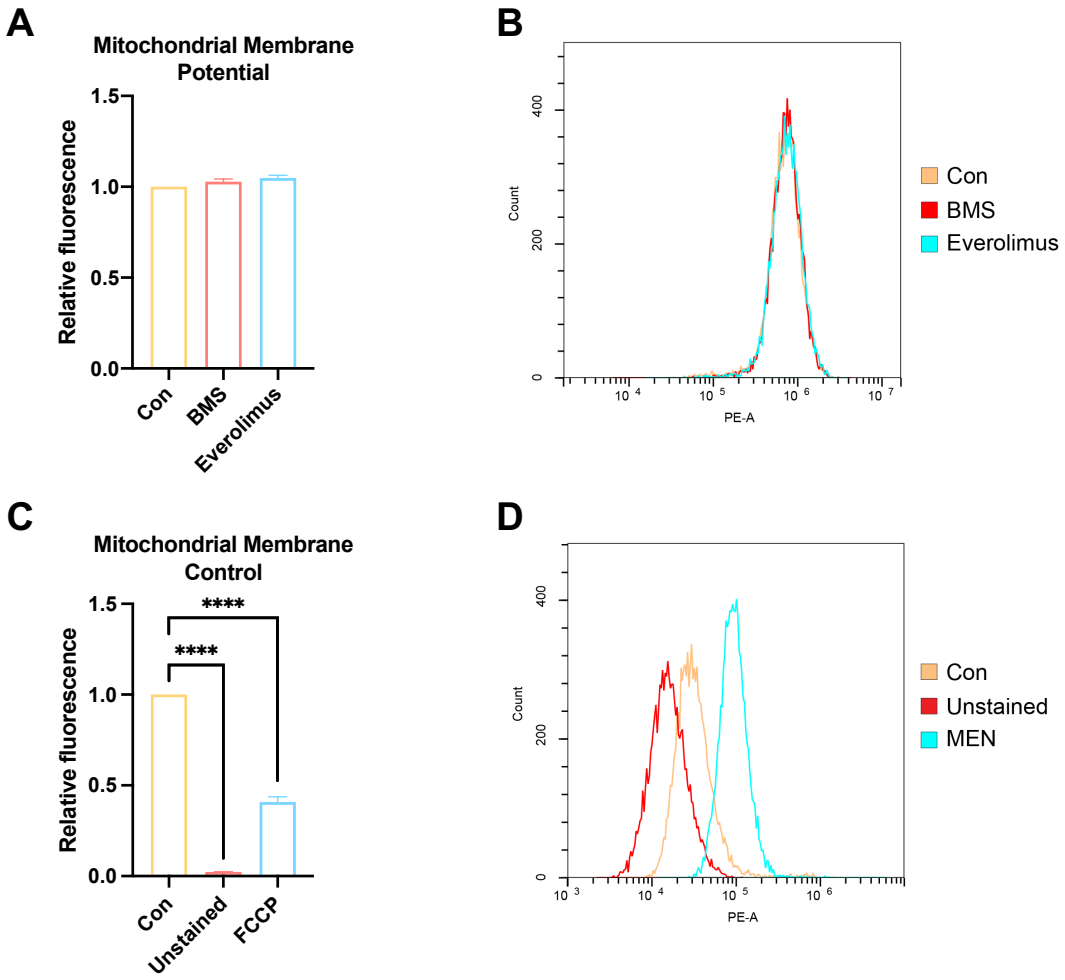

Figure 7. MRIs did not affect mitochondrial membrane potential.
Following 24 hours of culture in low-glucose (1g/L) media, MDA-MB-231 cells were treated with BMS-754807 (2.5μM) or everolimus (15.63nM) for 4 hours before being stained with tetramethylrhodamine (TMRM). Median fluorescence intensity **(A)** with representative frequency histogram of cellular fluorescence; decreased fluorescence indicates loss of mitochondrial membrane potential **(B)**. Mitochondrial membrane negative control achieved via p-trifluoromethoxy carbonyl cyanide phenyl hydrazone (FCCP) treatment combined with TMRM **(C)** with representative frequency histogram of cellular fluorescence **(D).** Data presented as mean ± SEM for n=3 experiments.

Metabolic reprogramming interventions enhance response to carboplatin

Having confirmed reprogramming of metabolic signaling, and limited alterations to mitochondrial function we next combined metabolic reprogramming agents were with carboplatin in MDA-MB-231 cells to examine if enhanced growth inhibition occurs when combining metabolic reprogramming agents with platinum chemotherapy, using carboplatin as the model for platinum chemotherapy. MDA-MB-231 cells were treated for 24 hours with BMS-754807 or everolimus before the addition of carboplatin for another 48 hours leading to 72 hours total of treatment time. MDA-MB-231 cells showed enhanced growth inhibition at increasing doses of carboplatin compared to control vehicle treated with DMSO (**Fig. 8A-B**).

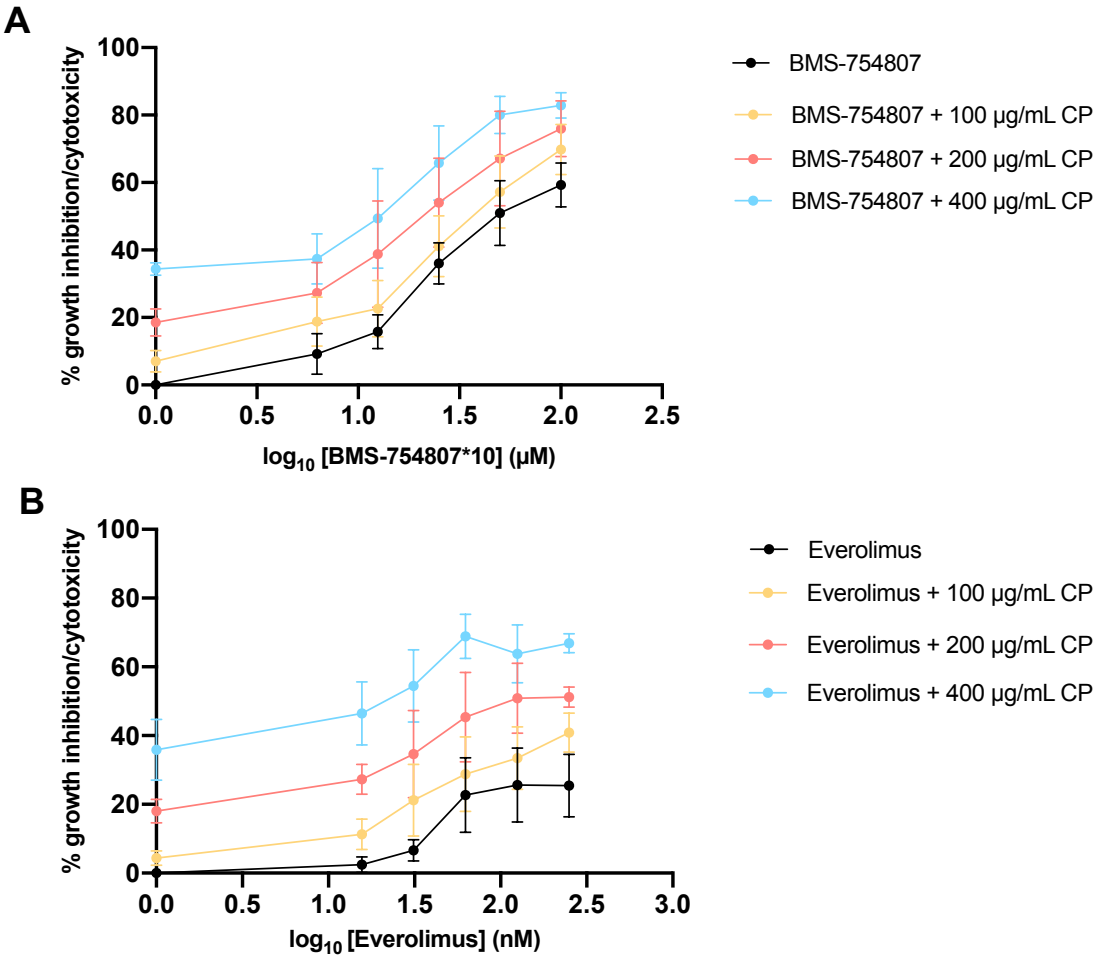

Figure 8. MRIs enhanced response to carboplatin.
Following 24 hours of nutrient restriction in low-glucose (1g/L) media, MDA-MB-231 cells were treated with BMS-754807 at increasing doses of 0.625, 1.25, 2.5, 5, and 10μM **(A)** or everolimus at increasing doses of 15.63, 31.25, 62.5, 125, and 250nM **(B)**. Following 24 hours of treatment, cells were also treated with 100, 200, or 400μg/mL carboplatin for an additional 48 hours. Vector controls for each group were treated with DMSO. An MTT assay was conducted to measure % growth inhibition/cytotoxicity. Data presented as mean ± SEM n=3 experiments.

To investigate whether the combination of everolimus or BMS-754807 with carboplatin was synergistic, we assayed our data for synergistic interaction[74]. A synergistic effect occurs where the response from two drugs together is greater than the predicted response from the two drugs individually. It can be determined as the excess of observed effect over expected effect as calculated by several synergy scoring

models. The Bliss independence model was used for analysis which assumes that the fractional response of two drugs in combination equals the sum of the two fractional responses of each drug minus their product. We used SynergyFinder to calculate Bliss independence for each concentration, and thus a synergy score for the combination of two drugs over an average of all dose combination cells. For example, a synergy score of 15 corresponds to 15% of response beyond expectation. There is no particular threshold to define synergy but SynergyFinder defines that a score less than -10 likely indicates an antagonistic interaction between two drugs, a score from -10 to 10 likely indicates an additive interaction between two drugs, and a score greater than 10 likely indicates a synergistic interaction between two drugs[75].

The combination of BMS-754807 and carboplatin produced a synergy score of 9.872 (**Fig. 9A**) while the combination of everolimus and carboplatin produced a synergy score of 9.354 (**Fig. 9B**). The highlighted boxes indicate the area where the most synergistic interaction is; for the combination of BMS-754807 with carboplatin, this occurs at a dose of 5μM BMS-754807 and 200μg/mL carboplatin. For the combination of everolimus with carboplatin, this occurs at a dose of 125nM everolimus and 200μg/mL carboplatin. These scores indicate an additive interaction between BMS-754807 or everolimus and carboplatin; however, they are close to the score of 10 threshold needed to define a synergistic interaction. Since SynergyFinder calculates its scores over the entire concentration range, this average may be a conservative estimate of the synergistic potential between the reagents. Thus, there is likely potential

that BMS-754807 or everolimus work synergistically with carboplatin at concentrations focused on the identified areas of optimal interaction.

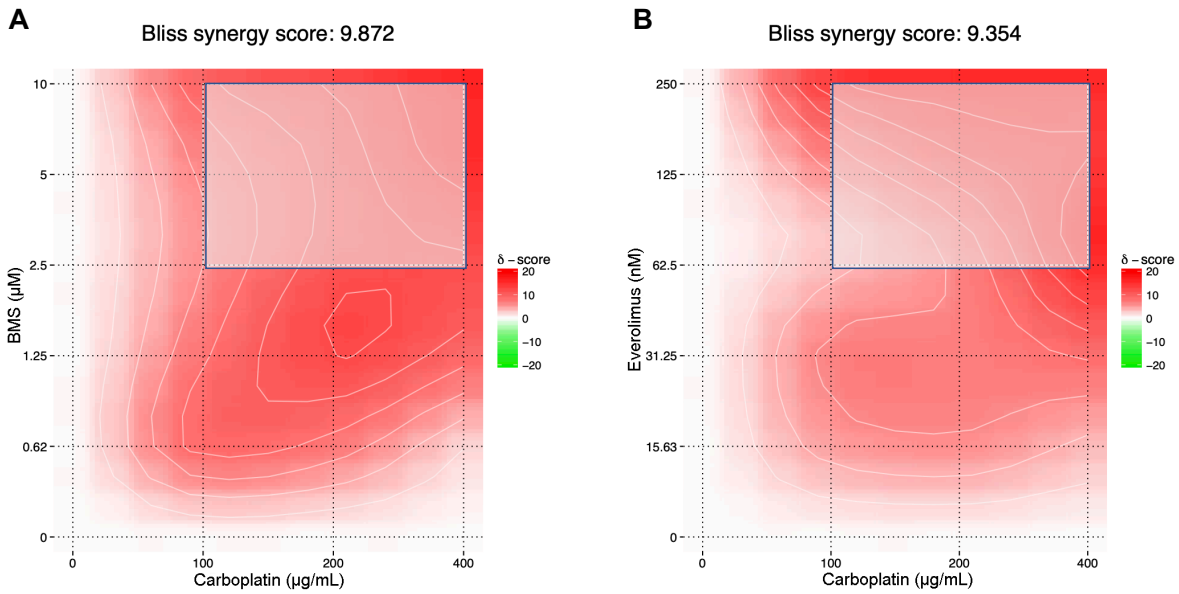

Figure 9. Analysis of synergistic potential of MRIs in combination with carboplatin.
Combination dose data of BMS-754807 and carboplatin analyzed utilizing SynergyFinder software with Bliss independence model. BMS-754807 in combination with carboplatin produced a Bliss synergy score of 9.872 **(A)** while everolimus in combination with carboplatin produced a Bliss synergy score of 9.354 **(B)**.

CHAPTER 3: AUTOPHAGY UNDERPINS SURVIVAL OF TNBC CELLS FOLLOWING METABOLIC REPROGRAMMING INTERVENTIONS INHIBITING IGF1R/IR OR MTORC1

Methods

MTT Assay

MDA-MB-231 cells were seeded ($1x10^4$ cells/well) in a 96-well plate overnight in glucose-restricted (1g/L) media for 24 hours, treated with either everolimus or BMS-754807 for 24 hours, and then treated with chloroquine for an additional 48 hours resulting in a 72-hour total treatment time. Media was aspirated and cells were incubated in a solution containing 3-(4,5-dimethylthiazol-2-yl)-2,5-diphenyltetrazolium bromide (MTT) (0.5 mg/mL) in PBS. After 1.5 hours. MTT reagent was removed and cells and precipitate solubilized with dimethyl sulfoxide (DMSO) and agitated on a plate shaker for 10 minutes. Absorbance was measured at 570 and 690 nm via a Cytation 3 Cell Imaging Reader (BioTek).

Flow Cytometry

MDA-MB-231 cells were seeded ($4.25x10^5$ cells/well) in a 6-well plate overnight in low-glucose (1g/L) media, then treated with BMS-754807 (2.5μM) or everolimus (15.63nM) for 4 hours. Cells were then trypsinized (Trypsin-EDTA, 0.25%, Gibco) and stained using CYTO-ID Autophagy Detection Kit (Enzo Life Sciences, #51031-0050) according to the manufacturer's protocol. Following 30 minutes of staining, data was acquired using a CytoFLEX flow cytometer (Beckman Coulter). Laser excitation at 488 nm was used to capture 10,000 live events for each sample.

Results

Metabolic reprogramming interventions do not alter autophagic activity in MDA-MB-231 cells

To analyze whether MDA-MB-231 TNBC cells treated with BMS-754807 or everolimus promote autophagy, cells were stained with CYTO-ID Green detection reagent which is a probe that fluoresces more brightly in vesicles produced during autophagy[76]. Staining with CYTO-ID Green detection reagent revealed an increase, although nonsignificant, in autophagic activity, ($p<0.01$) in MDA-MB-231 cells treated with BMS-754807 or everolimus compared to control (**Fig. 10A-B**). We confirmed the functioning of the assay by comparing cells stained with CYTO-ID Green detection reagent only to unstained cells for 30 min to confirm induction of signal (**Fig. 10C-D**).

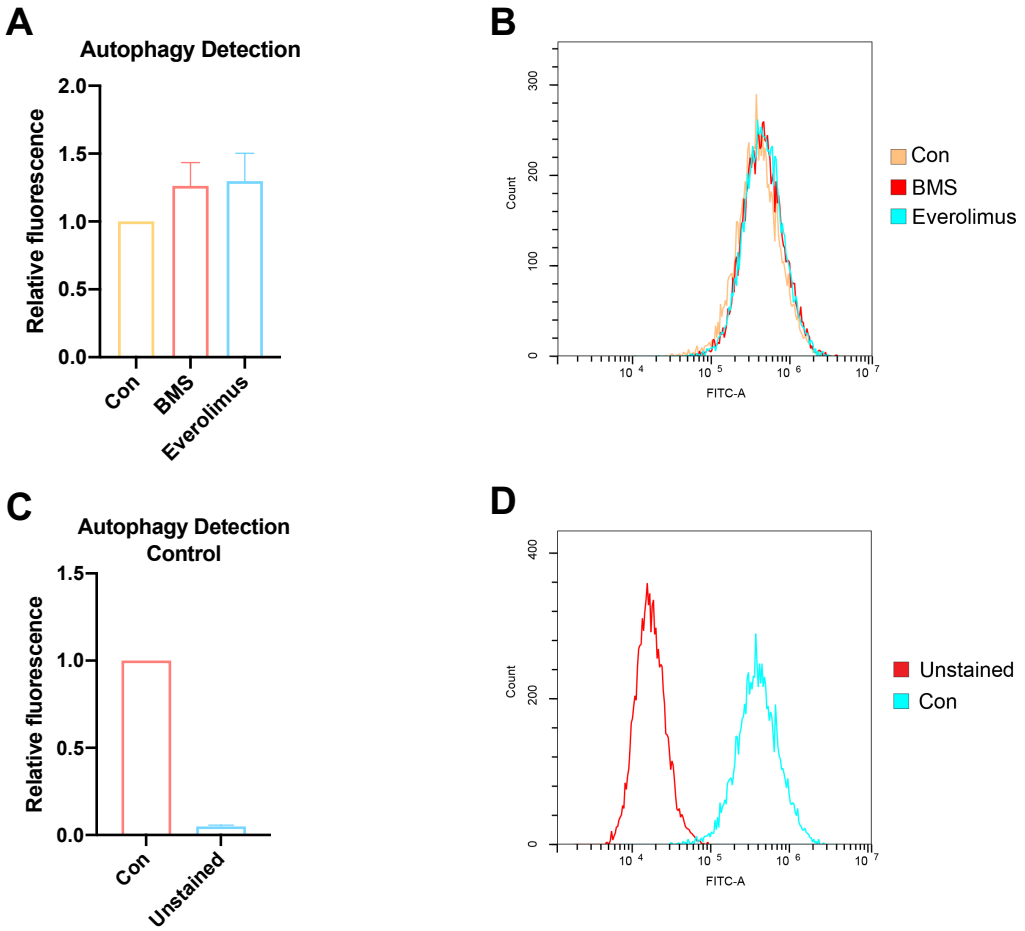

Figure 10. BMS-754807 and everolimus did not alter autophagic activity. Following 24 hours of culture in low-glucose (1g/L) media, MDA-MB-231 cells were treated with BMS-754807 (2.5μM) or everolimus (15.63nM) for 4 hours before being stained with CYTO-ID Green detection reagent. Median fluorescence intensity **(A)** with representative frequency histogram of cellular fluorescence; decreased fluorescence indicates loss of mitochondrial membrane potential **(B)**. Control compared to unstained control **(C)** with representative frequency histogram of cellular fluorescence **(D).** Data presented as mean ± SEM for n=3 experiments.

Metabolic reprogramming interventions used in combination with autophagy inhibition enhances cytotoxic effects of BMS-754707 or everolimus alone

Next, we examined the effect of chloroquine alone on the viability of MDA-MB-231 cells cultured under glucose-restricted (1g/L) conditions for 24 hours. Growth inhibition was assessed via MTT assay. Following 48 hours of treatment with chloroquine, MDA-MB-231 cells showed significant cytotoxicity at a 30μM dose ($p<0.01$) compared to control levels (**Fig. 11**).

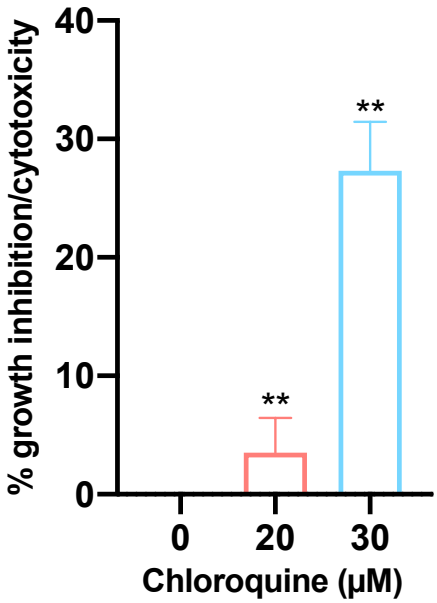

Figure 11. Chloroquine is cytotoxic in MDA-MB-231 cells.
Following 24 hours of nutrient restriction in low-glucose (1g/L) media, MDA-MB-231 cells were treated with chloroquine at 20 and 30μM ($p<0.01$). Control was low-glucose (1g/L) DMEM media. An MTT assay was conducted to measure % growth inhibition/cytotoxicity. Data presented as mean ± SEM n=3 experiments.

Chloroquine was next combined with BMS-754807 or everolimus in MDA-MB-231 cells to examine if enhanced growth inhibition occurs when combining metabolic reprogramming agents with autophagy inhibition. MDA-MB-231 cells were treated for 24 hours with BMS-754807 or everolimus before the addition of chloroquine for another 48 hours leading to 72 hours total of treatment time. Following treatment, MDA-MB-231 cells cultured in low-glucose media showed enhanced growth inhibition at increasing doses of chloroquine compared to control vehicle treated with DMSO (**Fig. 12A, 12B**).

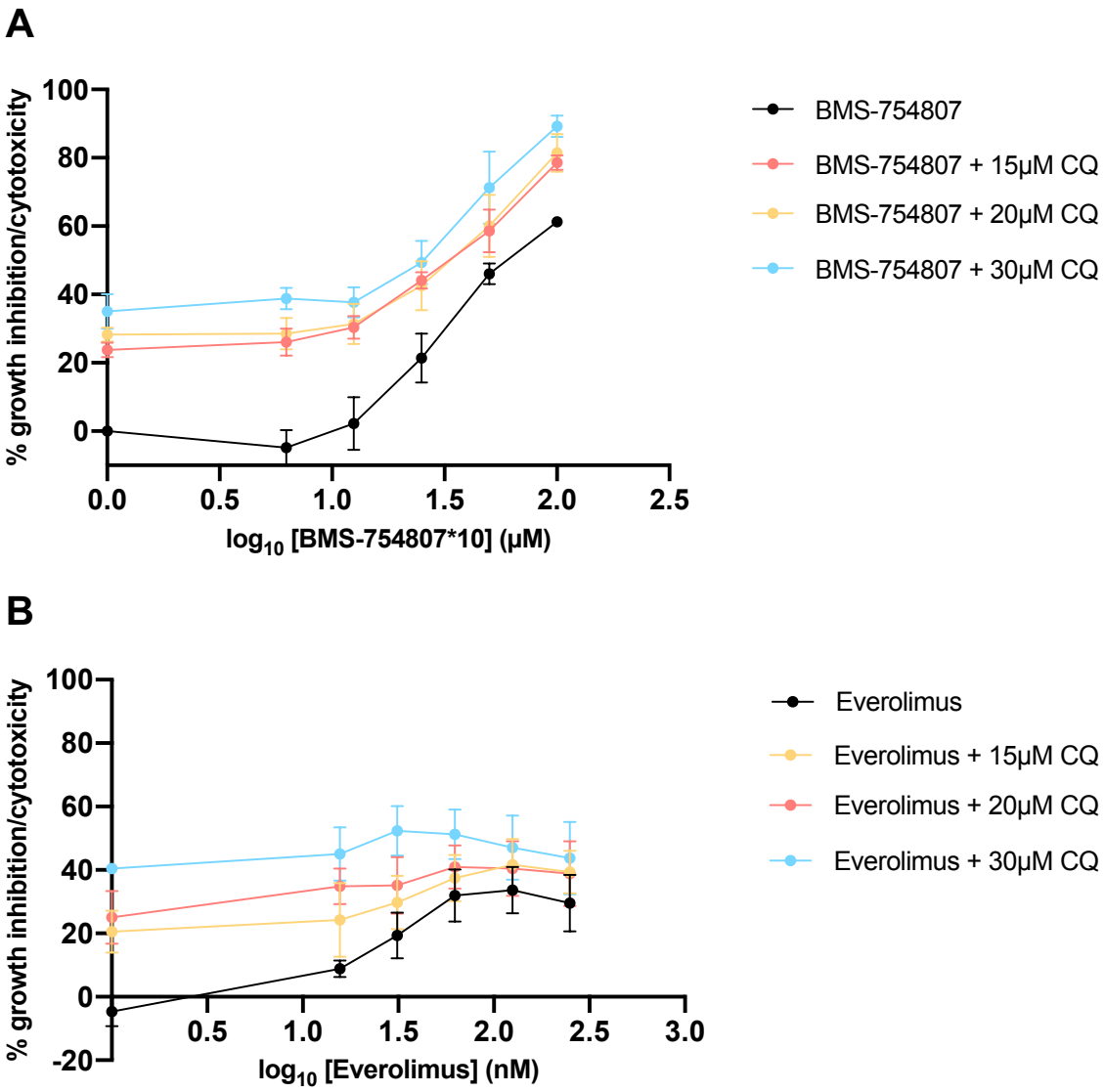

Figure 12. BMS-754807 enhanced response to chloroquine.
Following 24 hours of nutrient restriction in low-glucose (1g/L) media, MDA-MB-231 cells were treated with BMS-754807 at increasing doses of 0.625, 1.25, 2.5, 5, and 10μM **(A)** or everolimus at increasing doses of 15.63, 31.25, 62.5, 125, and 250nM **(B)**. Following 24 hours of treatment, cells were also treated with 0, 20, or 30μM chloroquine (CQ) for an additional 48 hours. Controls for each group were low-glucose (1g/L) DMEM media vector treated with DMSO. An MTT assay was conducted to measure % growth inhibition/cytotoxicity. Data presented as mean ± SEM for n=3 experiments.

To determine whether the combination of everolimus or BMS-754807 with chloroquine had a synergistic relationship, we again utilized SynergyFinder software to analyze synergistic potential via Bliss independence. The combination of BMS-754807

and chloroquine produced a synergy score of 9.592 (**Fig. 13A**), a score indicating an additive interaction between BMS-754807 and chloroquine. Again, the highlighted boxes indicate the area where the most synergistic interaction is; for the combination of BMS-754807 with chloroquine, this occurs at a dose of 0.625μM BMS-754807 and 15μM chloroquine. There is likely potential for greater synergy if examining only the effects closer to this optimal combination of BMS-754807 and chloroquine. For the combination of everolimus with chloroquine, this occurs at a dose of 125nM everolimus and 20μM chloroquine. Surprisingly, the combination of everolimus and chloroquine produced a synergy score of -7.122. (**Fig. 13B**), indicating that treatment of everolimus with chloroquine is less effective than predicted and that everolimus and chloroquine are inhibiting each other's cytotoxic effects.

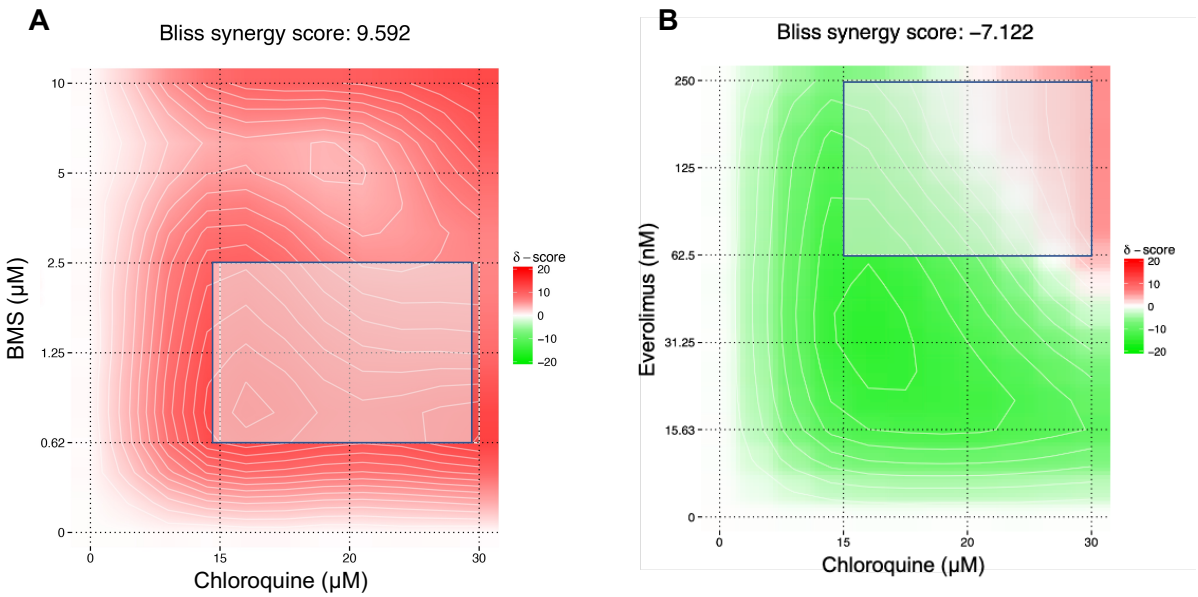

Figure 13. Analysis of synergistic potential of MRIs in combination with chloroquine.

Combination dose data of BMS-754807 or everolimus and carboplatin analyzed utilizing SynergyFinder software with Bliss independence model. BMS-754807 in combination with chloroquine produced a Bliss synergy score of 9.592 **(A)** while everolimus in combination with carboplatin produced a Bliss synergy score of -7.122 **(B)**.

CHAPTER 4: DISCUSSION AND FUTURE DIRECTIONS

Discussion

As TNBC is frequently associated with abnormalities in the PI3K/AKT/mTOR signaling cascade, the use of IGF-1/IGF-1R and mTORC1 inhibitors presents a promising avenue in TNBC therapy. Few clinical trials have investigated the use of the mTORC1 inhibitor, everolimus, in TNBC. A phase II neoadjuvant study conducted by Gonzalez et al. studied the use of paclitaxel treatment followed with fluorouracil, epirubicin, cyclophosphamide (FEC) regiment alone or in combination with everolimus treatment in 50 women with TNBC. They concluded that there was a higher clinical response in patients treated with everolimus, paclitaxel, and FEC compared to paclitaxel and FEC treatment only, though this response was nonsignificant[77]. Although everolimus has been used in treatment of other BC subtypes, there is very limited evidence of its use in combination with carboplatin or other platinum-based compounds. A clinical phase I/II trial recently conducted by Park et al. investigated the use gemcitabine and cisplatin (another platinum containing chemotherapy) in combination with everolimus compared to gemcitabine and cisplatin treatment alone in metastatic TNBC patients. Though they demonstrated that patients with TNBC had *PIK3CA* mutations in cell-free blood DNA samples, their findings showed that everolimus did not act synergistically with gemcitabine/cisplatin[78].

Early clinical trials proved ineffective when using IGF-1/IGF-1R inhibition as monotherapy against various cancer types. A phase II clinical trial investigating the use

of AXL1717, a small-molecule modulator of IGF-1R signaling, in non-small cell lung cancer found AXL1717 did not demonstrate significant benefit on progression-free or overall survival when used as a monotherapy[18]. Similarly, another study investigating the use of linsitinib, another IGF-1R inhibitor, on patients with relapsed small-cell lung cancer, found that although its use was safe, linsitinib did not demonstrate any useful clinical activity[19].

In this study, MDA-MB-231 TNBC cells were treated with BMS-754807 or everolimus to inhibit IGF-1/IGF-1R or mTORC1 respectively. Cells were cultured under low-glucose (1g/L) conditions to model and investigate response to treatment under conditions consistent with homeostatic glucose levels in a normoglycemic individual. Treatment of MDA-MB-231 cells with BMS-754807 or everolimus resulted in significant growth inhibition. One limitation of this study was everolimus's limited overall growth inhibition; however, similar results were observed *in vitro* by Ariaans et al. who found that everolimus lost its sensitivity in inhibiting MDA-MB-231 cell growth under low-glucose conditions. Overall, as expected, both BMS-754807 and everolimus resulted in significant growth inhibition, inducing metabolic stress and remodeling metabolism in TNBC cells.

Because treatment options for TNBC are limited, acquired chemoresistance presents an obstacle in TNBC therapy[67]. IGF-1R signaling has also been implicated in mediating resistance to chemotherapy in ovarian, breast, prostate, and bladder cancers[79]. Thus, IGF-1/IGF-1R and mTORC1 inhibition remains of particular interest in TNBC for its potential to restore chemosensitivity.

IGF-1R signaling has also been implicated in mediating resistance to platinum-based compounds as increased IGF-1R signaling has been shown to induce cisplatin resistance in ovarian cancer[80]. Furthermore, the PI3K/AKT signaling cascade has been implicated in mediating resistance to platinum-based compounds in both breast and ovarian cancer[81]. This study tested the hypothesis that IGF-1R/IR or mTORC1 inhibition enhances the response to platinum chemotherapy. Targeting the IGF-1R and mTORC1 pathways which are frequently dysregulated in TNBC, demonstrated effectiveness in combination with carboplatin. BMS-754807 and everolimus both worked additively with carboplatin to achieve growth-inhibitory effects. This is in agreement with a study conducted by Xu et al. in 2020 which investigated the effects of paclitaxel, a taxane which is commonly used as part of first-line therapy for BC, alone and in combination with everolimus on MDA-MB-231 TNBC cells[82]. Their work demonstrated that everolimus increases the antiproliferative effects of paclitaxel treatment alone through increased growth inhibition, the induction of apoptosis, and downregulated mTOR signaling[82]. One major limitation of this study is that the results achieved may have been a conservative estimate of the synergistic potential between BMS-754807 or everolimus with carboplatin. To fully investigate the potential of synergy between these drugs, further studies should utilize concentrations focused more narrowly on the identified areas of optimal interaction.

To further determine if BMS-754807 and everolimus reprogrammed cell metabolism, we analyzed mitochondrial mass, mitochondrial superoxide production, and mitochondrial membrane potential following treatment of MDA-MB-231 cells with BMS-754807 or everolimus. The results showed that treatment with BMS-754807, not

everolimus, led to a significant increase in mitochondrial mass compared to untreated cells which is in agreement with previous work conducted in the Hursting lab showing that MCF-7 BC cells exposed to BMS-754807 leads to a significant reduction in mitochondrial mass[83]. Although the mTOR complex has been shown to play an important role in regulating mitochondrial function and a study conducted by Schieke et al. demonstrated that treatment with rapamycin resulted in significantly reduced mitochondrial membrane potential, our results found that there was no significant difference in mitochondrial superoxide production or mitochondrial membrane potential following treatment with either BMS-754807 or everolimus[84,85]. Though our study did not show that treatment with BMS-754807 or everolimus resulted in significant mitochondrial effects, mitochondrial metabolism remains a promising area for cancer therapy. Mitochondrial metabolism plays a crucial role in generating ATP and TCA cycle intermediates which serve as precursors for the synthesis of macromolecules that can fuel cell growth and tumor proliferation[86]. On the other hand, cancer cells have the ability to switch between mitochondrial metabolism and glycolysis depending on nutrient status[87]. This metabolic flexibility is important as it has been associated with chemoresistance in cancer cells[88].

As dose-limiting toxicities during cytotoxic chemotherapy pose an obstacle to treatment due to the potential for the development of side effects including nausea, vomiting, gastrointestinal inflammation, and central/peripheral nervous system neurotoxicity, there is growing interest in other methods of remodeling cancer metabolism including dietary energy restriction[89]. For instance, fasting, calorie restriction, and the use of the ketogenic diet have all demonstrated antitumorigenic

benefits in rodent models[48,65,90]. Dietary energy restriction such as CR achieves its beneficial anticancer effects through several mechanisms including reduction/inactivation of growth factor signaling pathways such as the IGF-1 signaling cascade as well as decreased chronic inflammation and systemic leptin levels[50]. Importantly, obesity also results in metabolic remodeling through a constant state of hyperinsulinemia whereby growth hormone receptor and its related signaling cascades are upregulated leading to tumor growth and proliferation[50]. Obese patients with BC can develop chemoresistance to pharmacological/chemotherapeutic agents due to several factors including adipose tissue expansion resulting in increased pro-tumorigenic adipokines in addition to several other pro-survival factors[91].

In addition to dietary energy restriction, other metabolically directed agents have been used in combination with chemotherapy or other therapies to target cancer growth and progression. For instance, the IGF-1R inhibitor, picropodophyllin (PPP), has been used in combination with the FDA approved type II diabetes agent, metformin, and resulted in greater growth inhibition of endometrial cancer cells compared to either agent alone[92]. Furthermore, combination treatment of pemetrexed disodium, an antifolate agent, with cisplatin has shown promising results and has been well-tolerated in patients with advanced non-small cell lung cancer[93]. Thus, the use of combination approaches using pharmacological/chemotherapeutic interventions which target multiple pathways that maximize efficacy while minimizing harsh adverse effects continues to show promise in the prevention and treatment of cancer.

As tumors develop, cancer cells face increased proliferative demands even in a tumor microenvironment characterized by dysfunctional vascularization and hypoxia

while cells compete for a limited supply of nutrients. To cope with these stressful conditions, cancer cells often utilize autophagy to generate metabolic fuels presenting a potential target for improving response to cancer therapy[57]. Furthermore, increased autophagic activity following therapy has been implicated in chemoresistance across multiple breast cancer subtypes[94,95]. This leads to the potential for combination therapies using autophagy inhibitors with cytotoxic therapies to overcome chemotherapeutic resistance.

This study examined the hypothesis that BMS-754807 and everolimus and BMS-754807, as inhibitors of IGF-1R/IR and mTORC1 respectively, induce autophagy. Our results showed a nonsignificant increase in autophagic activity in MDA-MB-231 cells treated with BMS-754807 or everolimus compared to untreated cells. Our findings agree with the work of Dayyani et al. which demonstrated that treatment of prostate cancer cells with BMS-754807 did not result in significant amounts of the protein LC3-II, which allows for the quantification of autophagosomes, suggesting autophagy may play a limited role in survival of MDA-MB-231 cells following BMS-754807 treatment[96]. However, further experiments using higher concentrations of BMS-754807 and everolimus may be necessary in order to better visualize and measure autophagic flux within treated cells.

Next, we tested the hypothesis that autophagy underpins survival of MDA-MB-231 cells by targeting metabolic pathways known to be dysregulated in TNBC, specifically through inhibition of IGF-1R/IR and mTORC1, followed by treatment with the autophagy inhibitor, chloroquine. Our findings demonstrated that metabolic reprogramming interventions used in combination with autophagy inhibition enhances

the cytotoxic effects of MRIs alone. BMS-754807 and chloroquine worked additively to inhibit MDA-MB-231 cell growth; however, we found that chloroquine and everolimus inhibited each other's growth-inhibitory effects. A study conducted by Grimaldi et al. found that the combination of everolimus and chloroquine synergistically inhibited growth of endothelial progenitor cells[97]. Our findings do not agree with Grimaldi et al. as we did not find that the addition of chloroquine increased the growth-inhibitory effect of everolimus. However, as mentioned previously, a limitation of this study is that the results achieved may have been a conservative estimate of the synergistic potential between BMS-754807 or everolimus with chloroquine. Further experimentation using concentrations of BMS-754807 and chloroquine focused more narrowly on the identified areas of optimal interaction may reveal a true synergistic relationship between the two. This project is effective in informing future experiments that can further explore whether the combination of everolimus or BMS-754807 with chloroquine will be effective in TNBC treatment. Together, these studies highlight the potential of combining MRIs with carboplatin or chloroquine in triple-negative BC cells to improve current TNBC therapies.

One limitation of this study is that all experiments were conducted in a single cell line. Furthermore, all experiments were conducted in two-dimensional (2D) cell culture. While 2D cell culture where cancer cells are grown in a monolayer provides useful initial information about the effectiveness of pharmacological agents and chemotherapy treatment, three-dimensional (3D) cell culture more accurately mimic the *in vivo* tumor microenvironment. 2D cell culture leads to more flattened cell morphology and cell-cell and cell-extracellular environment interactions of cells grown in a monolayer do not

match those of cells in a 3D environment[98]. These changes can affect cellular function, intracellular cell structure, as well as cell signaling/secretion[99]. For these reasons, the development of 3D cell culture is useful as a more physiologically relevant model of the tumor microenvironment. Tumor spheroids have been shown to more faithfully recapitulate *in vivo* tumor cell metabolism and signaling within the PI3K/AKT/mTOR signaling cascade[100]. Thus, tumor spheroids can serve as a better predictor of drug response in solid tumors[100].

Lastly, these experiments were unable to assess toxicity in response to the pharmacological agents and chemotherapy used. Future experiments will explore the effects of MRIs and chemotherapy in a three-dimensional model of BC to confirm the efficacy of single agent and combination therapies and provide better prediction of *in vivo* response. MRIs that show efficacy in both two and three-dimensional analyses will then be tested in preclinical mouse models to confirm the effects of MRIs on factors such as metastasis and toxicity.

Three-dimensional *in vitro* analyses

Our proposed 3D cell culture model includes tumor spheroids grown under non-adherent conditions in a biologically relevant extracellular matrix to confirm the efficacy of single agent and combination therapies and provide better prediction of *in vivo* response. MDA-MB-231 cells will first be grown as a monolayer and then trysinized for seeding in ultra-low attachment plates in low-glucose DMEM. Tumor spheroids will be embedded in a Matrigel: type I collagen mixture (1:1). Following the treatment approach from the 2D cell culture model, spheroids will be treated with BMS-754807 or

everolimus for 24 hours followed by combination treatment with either carboplatin or chloroquine for 48 hours resulting in a 72-hour total treatment time.

Confirmation of target inhibition will be determined in un-embedded spheroids, which will undergo treatment for 4 hours with MRI alone or in combination with carboplatin or chloroquine. Spheroids will be collected using the Cultrex 3-D Culture Cell Harvesting Kit (Trevigen) for Western blotting. To analyze the extent of invasion of embedded spheroids into the surrounding extracellular environment, spheroids will be imaged using the ImageJ software.

Animal Design Protocol

Eight-week-old wild-type female C57BL/6J mice (Jackson Laboratories) will be allowed to acclimate for one week before randomization to either a purified high fat diet (60% kcal from fat) or a low-fat control diet (10% kcal from fat). Body weight will be measured weekly from diet start to study endpoint. Body composition measurements will be taken at baseline and at tumor cell injection via Magnetic Resonance Imaging (MRI) conducted by the UNC Animal Metabolism Phenotyping Core. Following 15 weeks on diet, E0771 cells (a C57BL/6 syngeneic line similar to MDA-MB-231) will be orthotopically injected into the 4^{th} mammary fat pad of lean and obese mice. Tumor growth will be measured twice weekly with calipers with longitudinal and transverse diameters recorded. Once 50% of tumors within each diet group reach appropriate size ($100mm^3$), mice will be randomized to the following treatment groups: 1) Vehicle-(saline) injected control, 2) Carboplatin only (20mg/kg twice weekly by intraperitoneal injection), 3) MRI (BMS-754807 or everolimus) + carboplatin. Doses for *in vivo* MRI analyses will be chosen based on previous studies showing safety and efficacy in murine models.

Blood glucose will be monitored to ensure no excessive toxicity arising from BMS-754807 treatment. Treatment will be given over a period of three weeks following a dosing schedule such as the one outlined below (**Table 1**):

Table 1. Proposed treatment schedule for single-agent and combination therapies

Day	1	2	3	4	5	6	7
Group 1: Vehicle	Vehicle	Vehicle		Vehicle	Vehicle		
Group 2: CP only	Vehicle	CP (20mg/kg)		Vehicle	CP (20mg/kg)		
Group 3: BMS + CP	BMS	BMS + CP		BMS	BMS + CP		

Planned Analysis

Upon completion of this study, animals will be sacrificed one week after the last treatment cycle or when any tumor reaches the IACAC defined maximum ($\geq$ 2cm in any dimension). Primary tumor progression will be reported as change in volume during treatment period, with *ex vivo* tumor volume reported in mm^3 and *ex vivo* tumor mass measured in mg. Tumors will be collected at sacrifice and a portion of each tumor frozen in liquid nitrogen for microarray analysis to identify differential expression of genes associated with metastasis and immune infiltration. Tumor histological sections will be examined via immunohistochemical (IHC) analysis. Lung and liver will be collected at sacrifice, and H&E-stained histological sections will be examined to assess metastatic burden. All histological outcomes will be conducted by the UNC Lineberger's Animal Histopathology Core.

CHAPTER 5: CONCLUSIONS

Project aims were designed to determine new approaches to treatment in triple-negative breast cancer, which exhibits elevated recurrence and metastasis rates and poorer overall survival compared to other breast cancer subtypes. It was hypothesized that MRIs which recapitulate the beneficial effects conferred by calorie restriction through inhibition of IGF-1R/IR and mTORC1 signaling sensitize TNBC cells to chemotherapy or autophagy inhibition. We determined that IGF-1R/IR and mTORC1 inhibition via BMS-754807 and everolimus respectively is potentially synergistic with carboplatin. Furthermore, we determined that BMS-754807 inhibits critical metabolism regulators in MDA-MB-231 TNBC cells and enhanced dependence on autophagy. However, further investigation is necessary to determine the optimal combinations of pharmacological agents with chemotherapy. Future experiments will explore the effects of MRIs and chemotherapy in a three-dimensional model of BC to confirm the efficacy of single agent and combination therapies and provide better prediction of *in vivo* response. MRIs that show efficacy in both two and three-dimensional analyses will be tested in preclinical mouse models to confirm the effects of MRIs on factors such as metastasis. Thus, this work will advance knowledge in bridging cellular and whole animal metabolism with cytotoxic chemotherapy to reduce TNBC mortality.

REFERENCES

1. Siegel RL, Miller KD, Fuchs HE, Jemal A. Cancer Statistics, 2021. *CA Cancer J Clin*. 2021;71(1):7-33. doi:10.3322/caac.21654

2. Bonotto M, Gerratana L, Poletto E, et al. Measures of Outcome in Metastatic Breast Cancer: Insights From a Real-World Scenario. *The Oncologist*. 2014;19(6):608-615. doi:10.1634/theoncologist.2014-0002

3. Lehmann BD, Bauer JA, Chen X, et al. Identification of human triple-negative breast cancer subtypes and preclinical models for selection of targeted therapies. *J Clin Invest*. 2011;121(7):2750-2767. doi:10.1172/JCI45014

4. Yin L, Duan J-J, Bian X-W, Yu S. Triple-negative breast cancer molecular subtyping and treatment progress. *Breast Cancer Res*. 2020;22(1):61. doi:10.1186/s13058-020-01296-5

5. Siddharth S, Sharma D. Racial Disparity and Triple-Negative Breast Cancer in African-American Women: A Multifaceted Affair between Obesity, Biology, and Socioeconomic Determinants. *Cancers*. 2018;10(12):514. doi:10.3390/cancers10120514

6. Massihnia D, Galvano A, Fanale D, et al. Triple negative breast cancer: shedding light onto the role of pi3k/akt/mtor pathway. *Oncotarget*. 2016;7(37):60712-60722. doi:10.18632/oncotarget.10858

7. Bianchini G, Balko JM, Mayer IA, Sanders ME, Gianni L. Triple-negative breast cancer: challenges and opportunities of a heterogeneous disease. *Nat Rev Clin Oncol*. 2016;13(11):674-690. doi:10.1038/nrclinonc.2016.66

8. Marra A, Trapani D, Viale G, Criscitiello C, Curigliano G. Practical classification of triple-negative breast cancer: intratumoral heterogeneity, mechanisms of drug resistance, and novel therapies. *Npj Breast Cancer*. 2020;6(1):54. doi:10.1038/s41523-020-00197-2

9. Isakoff SJ. Triple-Negative Breast Cancer: Role of Specific Chemotherapy Agents. *Cancer J*. 2010;16(1):53-61. doi:10.1097/PPO.0b013e3181d24ff7

10. Jhan J-R, Andrechek ER. Triple-negative breast cancer and the potential for targeted therapy. *Pharmacogenomics*. 2017;18(17):1595-1609. doi:10.2217/pgs-2017-0117

11. Ekyalongo RC, Yee D. Revisiting the IGF-1R as a breast cancer target. *NPJ Precis Oncol*. 2017;1. doi:10.1038/s41698-017-0017-y

12. Yu H. Role of the Insulin-Like Growth Factor Family in Cancer Development and Progression. *J Natl Cancer Inst*. 2000;92(18):1472-1489. doi:10.1093/jnci/92.18.1472

13. Laron Z. Insulin-like growth factor 1 (IGF-1): a growth hormone. *Mol Pathol MP*. 2001;54(5):311-316. doi:10.1136/mp.54.5.311

14. Baserga R, Peruzzi F, Reiss K. The IGF-1 receptor in cancer biology. *Int J Cancer*. 2003;107(6):873-877. doi:10.1002/ijc.11487

15. Christopoulos PF, Msaouel P, Koutsilieris M. The role of the insulin-like growth factor-1 system in breast cancer. *Mol Cancer*. 2015;14:43. doi:10.1186/s12943-015-0291-7

16. Larsson O, Girnita A, Girnita L. Role of insulin-like growth factor 1 receptor signalling in cancer. *Br J Cancer*. 2005;92(12):2097-2101. doi:10.1038/sj.bjc.6602627

17. Litzenburger BC, Creighton CJ, Tsimelzon A, et al. High IGF-IR Activity in Triple-Negative Breast Cancer Cell Lines and Tumorgrafts Correlates with Sensitivity to Anti–IGF-IR Therapy. *Clin Cancer Res*. 2011;17(8):2314-2327. doi:10.1158/1078-0432.CCR-10-1903

18. Bergqvist M, Holgersson G, Bondarenko I, et al. Phase II randomized study of the IGF-1R pathway modulator AXL1717 compared to docetaxel in patients with previously treated, locally advanced or metastatic non-small cell lung cancer. *Acta Oncol*. 2017;56(3):441-447. doi:10.1080/0284186X.2016.1253866

19. Chiappori AA, Otterson GA, Dowlati A, et al. A Randomized Phase II Study of Linsitinib (OSI-906) Versus Topotecan in Patients With Relapsed Small-Cell Lung Cancer. *The Oncologist*. 2016;21(10):1163. doi:10.1634/theoncologist.2016-0220

20. Saxton RA, Sabatini DM. mTOR Signaling in Growth, Metabolism, and Disease. *Cell*. 2017;168(6):960-976. doi:10.1016/j.cell.2017.02.004

21. Jhanwar-Uniyal M, Wainwright JV, Mohan AL, et al. Diverse signaling mechanisms of mTOR complexes: mTORC1 and mTORC2 in forming a formidable relationship. *Adv Biol Regul*. 2019;72:51-62. doi:10.1016/j.jbior.2019.03.003

22. Kim LC, Cook RS, Chen J. mTORC1 and mTORC2 in cancer and the tumor microenvironment. *Oncogene*. 2017;36(16):2191-2201. doi:10.1038/onc.2016.363

23. Ricoult SJH, Yecies JL, Ben-Sahra I, Manning BD. Oncogenic PI3K and K-Ras stimulate de novo lipid synthesis through mTORC1 and SREBP. *Oncogene*. 2016;35(10):1250-1260. doi:10.1038/onc.2015.179

24. Efeyan A, Sabatini DM. mTOR and cancer: many loops in one pathway. *Curr Opin Cell Biol*. 2010;22(2):169-176. doi:10.1016/j.ceb.2009.10.007

25. Yang G, Murashige DS, Humphrey SJ, James DE. A Positive Feedback Loop between Akt and mTORC2 via SIN1 Phosphorylation. *Cell Rep*. 2015;12(6):937-943. doi:10.1016/j.celrep.2015.07.016

26. Wang X, Proud CG. mTORC2 is a tyrosine kinase. *Cell Res*. 2016;26(1):1-2. doi:10.1038/cr.2015.134

27. Lee JJ, Loh K, Yap Y-S. PI3K/Akt/mTOR inhibitors in breast cancer. *Cancer Biol Med*. 2015;12(4):342-354. doi:10.7497/j.issn.2095-3941.2015.0089

28. O'Reilly KE, Rojo F, She Q-B, et al. mTOR Inhibition Induces Upstream Receptor Tyrosine Kinase Signaling and Activates Akt. *Cancer Res*. 2006;66(3):1500-1508. doi:10.1158/0008-5472.CAN-05-2925

29. Ward ZJ, Bleich SN, Cradock AL, et al. Projected U.S. State-Level Prevalence of Adult Obesity and Severe Obesity. *N Engl J Med*. 2019;381(25):2440-2450. doi:10.1056/NEJMsa1909301

30. Rock CL, Thomson C, Gansler T, et al. American Cancer Society guideline for diet and physical activity for cancer prevention. *CA Cancer J Clin*. 2020;70(4):245-271. doi:10.3322/caac.21591

31. Pierobon M, Frankenfeld CL. Obesity as a risk factor for triple-negative breast cancers: a systematic review and meta-analysis. *Breast Cancer Res Treat*. 2013;137(1):307-314. doi:10.1007/s10549-012-2339-3

32. Phipps AI, Chlebowski RT, Prentice R, et al. Body size, physical activity, and risk of triple-negative and estrogen receptor-positive breast cancer. *Cancer Epidemiol Biomark Prev Publ Am Assoc Cancer Res Cosponsored Am Soc Prev Oncol*. 2011;20(3):454-463. doi:10.1158/1055-9965.EPI-10-0974

33. Picon-Ruiz M, Morata-Tarifa C, Valle-Goffin JJ, Friedman ER, Slingerland JM. Obesity and adverse breast cancer risk and outcome: Mechanistic insights and strategies for intervention: Breast Cancer, Inflammation, and Obesity. *CA Cancer J Clin*. 2017;67(5):378-397. doi:10.3322/caac.21405

34. Copson ER, Cutress RI, Maishman T, et al. Obesity and the outcome of young breast cancer patients in the UK: the POSH study. *Ann Oncol Off J Eur Soc Med Oncol*. 2015;26(1):101-112. doi:10.1093/annonc/mdu509

35. Malley CO, Pidgeon GP. The mTOR pathway in obesity driven gastrointestinal cancers: Potential targets and clinical trials. *BBA Clin*. 2016;5:29-40. doi:10.1016/j.bbacli.2015.11.003

36. Khandekar MJ, Cohen P, Spiegelman BM. Molecular mechanisms of cancer development in obesity. *Nat Rev Cancer*. 2011;11(12):886-895. doi:10.1038/nrc3174

37. Renehan AG, Zwahlen M, Egger M. Adiposity and cancer risk: new mechanistic insights from epidemiology. *Nat Rev Cancer*. 2015;15(8):484-498. doi:10.1038/nrc3967

38. Chen C-T, Du Y, Yamaguchi H, et al. Targeting the IKKβ/mTOR/VEGF Signaling Pathway as a Potential Therapeutic Strategy for Obesity-Related Breast Cancer. *Mol Cancer Ther*. 2012;11(10):2212-2221. doi:10.1158/1535-7163.MCT-12-0180

39. Dietze EC, Chavez TA, Seewaldt VL. Obesity and Triple-Negative Breast Cancer: Disparities, Controversies, and Biology. *Am J Pathol*. 2018;188(2):280-290. doi:10.1016/j.ajpath.2017.09.018

40. Hartman ZC, Poage GM, den Hollander P, et al. Growth of triple-negative breast cancer cells relies upon coordinate autocrine expression of the proinflammatory cytokines IL-6 and IL-8. *Cancer Res*. 2013;73(11):3470-3480. doi:10.1158/0008-5472.CAN-12-4524-T

41. O'Flanagan CH, Smith LA, McDonell SB, Hursting SD. When less may be more: calorie restriction and response to cancer therapy. *BMC Med*. 2017;15(1):106. doi:10.1186/s12916-017-0873-x

42. Longo VD, Fontana L. Calorie restriction and cancer prevention: metabolic and molecular mechanisms. *Trends Pharmacol Sci*. 2010;31(2):89-98. doi:10.1016/j.tips.2009.11.004

43. Mattison JA, Colman RJ, Beasley TM, et al. Caloric restriction improves health and survival of rhesus monkeys. *Nat Commun*. 2017;8:14063. doi:10.1038/ncomms14063

44. Harvey AE, Lashinger LM, Otto G, Nunez NP, Hursting SD. Decreased systemic IGF-1 in response to calorie restriction modulates murine tumor cell growth, nuclear factor-κB activation, and inflammation-related gene expression: CALORIE RESTRICTION, NF-κB AND COLON CANCER. *Mol Carcinog*. 2013;52(12):997-1006. doi:10.1002/mc.21940

45. Simone BA, Champ CE, Rosenberg AL, et al. Selectively starving cancer cells through dietary manipulation: methods and clinical implications. *Future Oncol*. 2013;9(7):959-976. doi:10.2217/fon.13.31

46. Nencioni A, Caffa I, Cortellino S, Longo VD. Fasting and cancer: molecular mechanisms and clinical application. *Nat Rev Cancer*. 2018;18(11):707-719. doi:10.1038/s41568-018-0061-0

47. Lee C, Longo VD. Fasting vs dietary restriction in cellular protection and cancer treatment: from model organisms to patients. *Oncogene*. 2011;30(30):3305-3316. doi:10.1038/onc.2011.91

48. de Groot S, Vreeswijk MPG, Welters MJP, et al. The effects of short-term fasting on tolerance to (neo) adjuvant chemotherapy in HER2-negative breast cancer patients: a randomized pilot study. *BMC Cancer*. 2015;15:652. doi:10.1186/s12885-015-1663-5

49. Ingram DK, de Cabo R. Calorie restriction in rodents: Caveats to consider. *Ageing Res Rev*. 2017;39:15-28. doi:10.1016/j.arr.2017.05.008

50. Hursting SD, Dunlap SM, Ford NA, Hursting MJ, Lashinger LM. Calorie restriction and cancer prevention: a mechanistic perspective. *Cancer Metab*. 2013;1(1):10. doi:10.1186/2049-3002-1-10

51. Motzer RJ, Escudier B, Oudard S, et al. Efficacy of everolimus in advanced renal cell carcinoma: a double-blind, randomised, placebo-controlled phase III trial. *The Lancet*. 2008;372(9637):449-456. doi:10.1016/S0140-6736(08)61039-9

52. Pavel ME, Hainsworth JD, Baudin E, et al. Everolimus plus octreotide long-acting repeatable for the treatment of advanced neuroendocrine tumours associated with carcinoid syndrome (RADIANT-2): a randomised, placebo-controlled, phase 3 study. *The Lancet*. 2011;378(9808):2005-2012. doi:10.1016/S0140-6736(11)61742-X

53. Royce M, Bachelot T, Villanueva C, et al. Everolimus Plus Endocrine Therapy for Postmenopausal Women With Estrogen Receptor-Positive, Human Epidermal Growth Factor Receptor 2-Negative Advanced Breast Cancer: A Clinical Trial. *JAMA Oncol*. 2018;4(7):977-984. doi:10.1001/jamaoncol.2018.0060

54. Yunokawa M, Koizumi F, Kitamura Y, et al. Efficacy of everolimus, a novel mTOR inhibitor, against basal-like triple-negative breast cancer cells. *Cancer Sci*. 2012;103(9):1665-1671. doi:10.1111/j.1349-7006.2012.02359.x

55. Carboni JM, Wittman M, Yang Z, et al. BMS-754807, a small molecule inhibitor of insulin-like growth factor-1R/IR. *Mol Cancer Ther*. 2009;8(12):3341-3349. doi:10.1158/1535-7163.MCT-09-0499

56. Awasthi N, Zhang C, Ruan W, Schwarz MA, Schwarz RE. BMS-754807, a Small-Molecule Inhibitor of Insulin-like Growth Factor-1 Receptor/Insulin Receptor, Enhances Gemcitabine Response in Pancreatic Cancer. *Mol Cancer Ther*. 2012;11(12):2644-2653. doi:10.1158/1535-7163.MCT-12-0447

57. Levy JMM, Towers CG, Thorburn A. Targeting autophagy in cancer. *Nat Rev Cancer*. 2017;17(9):528-542. doi:10.1038/nrc.2017.53

58. Kondo Y, Kanzawa T, Sawaya R, Kondo S. The role of autophagy in cancer development and response to therapy. *Nat Rev Cancer*. 2005;5(9):726-734. doi:10.1038/nrc1692

59. White E. The role for autophagy in cancer. *J Clin Invest*. 2015;125(1):42-46. doi:10.1172/JCI73941

60. Mathew R, Karantza-Wadsworth V, White E. Role of autophagy in cancer. *Nat Rev Cancer*. 2007;7(12):961-967. doi:10.1038/nrc2254

61. Rebecca VW, Amaravadi RK. Emerging strategies to effectively target autophagy in cancer. *Oncogene*. 2016;35(1):1-11. doi:10.1038/onc.2015.99

62. Pietrocola F, Pol J, Vacchelli E, et al. Caloric Restriction Mimetics Enhance Anticancer Immunosurveillance. *Cancer Cell*. 2016;30(1):147-160. doi:10.1016/j.ccell.2016.05.016

63. Mulcahy Levy JM, Thorburn A. Autophagy in cancer: moving from understanding mechanism to improving therapy responses in patients. *Cell Death Differ*. 2020;27(3):843-857. doi:10.1038/s41418-019-0474-7

64. Xia H, Green DR, Zou W. Autophagy in tumour immunity and therapy. *Nat Rev Cancer*. Published online March 23, 2021. doi:10.1038/s41568-021-00344-2

65. Lashinger LM, O'Flanagan CH, Dunlap SM, et al. Starving cancer from the outside and inside: separate and combined effects of calorie restriction and autophagy inhibition on Ras-driven tumors. *Cancer Metab*. 2016;4(1):18. doi:10.1186/s40170-016-0158-4

66. Amaravadi RK, Yu D, Lum JJ, et al. Autophagy inhibition enhances therapy-induced apoptosis in a Myc-induced model of lymphoma. *J Clin Invest*. 2007;117(2):326-336. doi:10.1172/JCI28833

67. Kim C, Gao R, Sei E, et al. Chemoresistance Evolution in Triple-Negative Breast Cancer Delineated by Single-Cell Sequencing. *Cell*. 2018;173(4):879-893.e13. doi:10.1016/j.cell.2018.03.041

68. Chittaranjan S, Bortnik S, Dragowska WH, et al. Autophagy Inhibition Augments the Anticancer Effects of Epirubicin Treatment in Anthracycline-Sensitive and -Resistant Triple-Negative Breast Cancer. *Clin Cancer Res*. 2014;20(12):3159-3173. doi:10.1158/1078-0432.CCR-13-2060

69. NIH. Analyzing Electrophoretic Gels. Accessed February 28, 2021. https://imagej.nih.gov/nih-image/manual/tech.html

70. Kumar P, Nagarajan A, Uchil PD. Analysis of Cell Viability by the MTT Assay. *Cold Spring Harb Protoc*. 2018;2018(6):pdb.prot095505. doi:10.1101/pdb.prot095505

71. Doherty E, Perl A. Measurement of Mitochondrial Mass by Flow Cytometry during Oxidative Stress. *React Oxyg Species Apex NC*. 2017;4(10):275-283. doi:10.20455/ros.2017.839

72. Kauffman ME, Kauffman MK, Traore K, et al. MitoSOX-Based Flow Cytometry for Detecting Mitochondrial ROS. *React Oxyg Species Apex NC*. 2016;2(5):361-370. doi:10.20455/ros.2016.865

73. ThermoFisher Scientific. Assays for Mitochondria Function. Accessed March 10, 2021. https://www.thermofisher.com/us/en/home/life-science/cell-analysis/cell-viability-and-regulation/apoptosis/mitochondria-function.html#MitoSoxRedMSI

74. Roell KR, Reif DM, Motsinger-Reif AA. An Introduction to Terminology and Methodology of Chemical Synergy—Perspectives from Across Disciplines. *Front Pharmacol*. 2017;8:158. doi:10.3389/fphar.2017.00158

75. Ianevski A, He L, Aittokallio T, Tang J. SynergyFinder: a web application for analyzing drug combination dose-response matrix data. *Bioinforma Oxf Engl*. 2017;33(15):2413-2415. doi:10.1093/bioinformatics/btx162

76. Guo S, Liang Y, Murphy SF, et al. A rapid and high content assay that measures cyto-ID-stained autophagic compartments and estimates autophagy flux with potential

clinical applications. *Autophagy*. 2015;11(3):560-572. doi:10.1080/15548627.2015.1017181

77. Gonzalez-Angulo AM, Akcakanat A, Liu S, et al. Open-label randomized clinical trial of standard neoadjuvant chemotherapy with paclitaxel followed by FEC versus the combination of paclitaxel and everolimus followed by FEC in women with triple receptor-negative breast cancer. *Ann Oncol*. 2014;25(6):1122-1127. doi:10.1093/annonc/mdu124

78. Park IH, Kong S-Y, Kwon Y, et al. Phase I/II clinical trial of everolimus combined with gemcitabine/cisplatin for metastatic triple-negative breast cancer. *J Cancer*. 2018;9(7):1145-1151. doi:10.7150/jca.24035

79. Yuan J, Yin Z, Tao K, Wang G, Gao J. Function of insulin-like growth factor 1 receptor in cancer resistance to chemotherapy. *Oncol Lett*. 2018;15(1):41-47. doi:10.3892/ol.2017.7276

80. Eckstein N, Servan K, Hildebrandt B, et al. Hyperactivation of the Insulin-like Growth Factor Receptor I Signaling Pathway Is an Essential Event for Cisplatin Resistance of Ovarian Cancer Cells. *Cancer Res*. 2009;69(7):2996-3003. doi:10.1158/0008-5472.CAN-08-3153

81. Eckstein N. Platinum resistance in breast and ovarian cancer cell lines. *J Exp Clin Cancer Res*. 2011;30(1):91. doi:10.1186/1756-9966-30-91

82. Xu T, Liu P, Li Q, Shi C, Wang X. Inhibitory effects of everolimus in combination with paclitaxel on adriamycin-resistant breast cancer cell line MDA-MB-231. *Taiwan J Obstet Gynecol*. 2020;59(6):828-834. doi:10.1016/j.tjog.2020.09.008

83. Lyons A, Coleman M, Riis S, et al. Insulin-like growth factor 1 signaling is essential for mitochondrial biogenesis and mitophagy in cancer cells. *J Biol Chem*. 2017;292(41):16983-16998. doi:10.1074/jbc.M117.792838

84. Schieke SM, Phillips D, McCoy JP, et al. The Mammalian Target of Rapamycin (mTOR) Pathway Regulates Mitochondrial Oxygen Consumption and Oxidative Capacity. *J Biol Chem*. 2006;281(37):27643-27652. doi:10.1074/jbc.M603536200

85. Morita M, Gravel S-P, Hulea L, et al. mTOR coordinates protein synthesis, mitochondrial activity and proliferation. *Cell Cycle Georget Tex*. 2015;14(4):473-480. doi:10.4161/15384101.2014.991572

86. Weinberg SE, Chandel NS. Targeting mitochondria metabolism for cancer therapy. *Nat Chem Biol*. 2015;11(1):9-15. doi:10.1038/nchembio.1712

87. Porporato PE, Filigheddu N, Pedro JMB-S, Kroemer G, Galluzzi L. Mitochondrial metabolism and cancer. *Cell Res*. 2018;28(3):265-280. doi:10.1038/cr.2017.155

88. Guerra F, Arbini AA, Moro L. Mitochondria and cancer chemoresistance. *Biochim Biophys Acta BBA - Bioenerg*. 2017;1858(8):686-699. doi:10.1016/j.bbabio.2017.01.012

89. Nurgali K, Jagoe RT, Abalo R. Editorial: Adverse Effects of Cancer Chemotherapy: Anything New to Improve Tolerance and Reduce Sequelae? *Front Pharmacol*. 2018;9:245. doi:10.3389/fphar.2018.00245

90. Otto C, Kaemmerer U, Illert B, et al. Growth of human gastric cancer cells in nude mice is delayed by a ketogenic diet supplemented with omega-3 fatty acids and medium-chain triglycerides. *BMC Cancer*. 2008;8(1):122. doi:10.1186/1471-2407-8-122

91. Lashinger LM, Rossi EL, Hursting SD. Obesity and Resistance to Cancer Chemotherapy: Interacting Roles of Inflammation and Metabolic Dysregulation. *Clin Pharmacol Ther*. 2014;96(4):458-463. doi:10.1038/clpt.2014.136

92. Xie Y, Wang J-L, Ji M, et al. Regulation of insulin-like growth factor signaling by metformin in endometrial cancer cells. *Oncol Lett*. 2014;8(5):1993-1999. doi:10.3892/ol.2014.2466

93. Shepherd FA, Dancey J, Arnold A, et al. Phase II study of pemetrexed disodium, a multitargeted antifolate, and cisplatin as first-line therapy in patients with advanced nonsmall cell lung carcinoma: a study of the National Cancer Institute of Canada Clinical Trials Group. *Cancer*. 2001;92(3):595-600. doi:10.1002/1097-0142(20010801)92:3<595::aid-cncr1359>3.0.co;2-d

94. Cufí S, Vazquez-Martin A, Oliveras-Ferraros C, et al. The anti-malarial chloroquine overcomes primary resistance and restores sensitivity to trastuzumab in HER2-positive breast cancer. *Sci Rep*. 2013;3:2469. doi:10.1038/srep02469

95. Chen S, Zhu X, Qiao H, et al. Protective autophagy promotes the resistance of HER2-positive breast cancer cells to lapatinib. *Tumour Biol J Int Soc Oncodevelopmental Biol Med*. 2016;37(2):2321-2331. doi:10.1007/s13277-015-3800-9

96. Dayyani F, Parikh NU, Varkaris AS, et al. Combined Inhibition of IGF-1R/IR and Src family kinases enhances antitumor effects in prostate cancer by decreasing activated survival pathways. *PloS One*. 2012;7(12):e51189. doi:10.1371/journal.pone.0051189

97. Grimaldi A, Balestrieri ML, D'Onofrio N, et al. The synergistic effect of everolimus and chloroquine on endothelial cell number reduction is paralleled by increased apoptosis and reduced autophagy occurrence. *PloS One*. 2013;8(11):e79658. doi:10.1371/journal.pone.0079658

98. Vidi P-A, Bissell MJ, Lelièvre SA. Three-Dimensional Culture of Human Breast Epithelial Cells: The How and the Why. In: Randell SH, Fulcher ML, eds. *Epithelial Cell Culture Protocols*. Vol 945. Methods in Molecular Biology. Humana Press; 2012:193-219. doi:10.1007/978-1-62703-125-7_13

99. Kapałczyńska M, Kolenda T, Przybyła W, et al. 2D and 3D cell cultures - a comparison of different types of cancer cell cultures. *Arch Med Sci AMS*. 2018;14(4):910-919. doi:10.5114/aoms.2016.63743

100. Riedl A, Schlederer M, Pudelko K, et al. Comparison of cancer cells in 2D vs 3D culture reveals differences in AKT–mTOR–S6K signaling and drug responses. *J Cell Sci*. 2017;130(1):203-218. doi:10.1242/jcs.188102